

Data-Driven Nested Stochastic Robust Optimization: A General Computational Framework and Algorithm for Optimization under Uncertainty in the Big Data Era

Chao Ning, Fengqi You*

Cornell University, Ithaca, New York 14853, USA

Abstract

A novel data-driven nested stochastic robust optimization (DDNSRO) framework is proposed to systematically and automatically handle labeled multi-class uncertainty data in optimization problems. Uncertainty realizations in large datasets are often collected from various conditions, which are encoded by class labels. A group of Dirichlet process mixture models is employed for uncertainty modeling from the multi-class uncertainty data. The proposed data-driven nonparametric uncertainty model could automatically adjust its complexity based on the data structure and complexity, thus accurately capturing the uncertainty information. A DDNSRO framework is further proposed based on the data-driven uncertainty model through a bi-level optimization structure. The outer optimization problem follows a two-stage stochastic programming approach to optimize the expected objective across different classes of data; robust optimization is nested as the inner problem to ensure the robustness of the solution while maintaining computational tractability. A tailored column-and-constraint generation algorithm is further developed to solve the resulting multi-level optimization problem efficiently. Case studies on strategic planning of process networks are presented to demonstrate the applicability of the proposed framework.

Key words: big data, optimization under uncertainty, Bayesian nonparametric model, column-and-constraint generation algorithm, process design and operations

*Corresponding author. Phone: (607) 255-1162; Fax: (607) 255-9166; E-mail: fengqi.you@cornell.edu

Introduction

In recent years, optimization under uncertainty has attracted tremendous attention from both academia and industry.¹⁻⁴ Uncertain parameters, if not being accounted for, could render the solution of an optimization problem suboptimal or even infeasible.⁵ To this end, a plethora of mathematical programming techniques, such as stochastic programming and robust optimization,⁶⁻⁸ have been proposed to support decision making under uncertainty. These techniques have their respective strengths and weaknesses, which lead to different application scopes.⁹⁻¹⁶ Stochastic programming focuses on the expected performance of a solution by leveraging the scenarios of uncertainty realization and their probability distribution.¹⁷⁻¹⁹ However, this approach requires accurate information on uncertainty probability distribution, and the resulting optimization problem could become computationally challenging as the number of scenarios increases.²⁰⁻²² Robust optimization provides an alternative paradigm that does not require accurate knowledge on probability distributions of uncertain parameters.²³⁻²⁶ It has attracted considerable interest owing to the merit of a good balance between solution quality, feasibility and computational tractability.²⁶ Nevertheless, robust optimization does not take advantage of available probability distribution information, and its solution usually suffers from the conservatism issue.²⁷ The state-of-the-art approaches for optimization under uncertainty leverage the synergy of different optimization methods to inherit their corresponding strengths and complement respective weaknesses.²⁸⁻³⁰ However, these approaches fall short of leveraging uncertainty data to facilitate the decision making processes. Due to massive amount of uncertainty data that can be collected and recent advances in machine learning techniques,³¹ data-driven optimization under uncertainty emerges as a promising paradigm.³²⁻³⁵ Therefore, the goal of this work is to propose a novel data-driven optimization framework that organically integrates uncertainty data information with the state-of-the-art optimization approach for data-driven decision-making under uncertainty.

There are a number of research challenges towards a general data-driven framework for optimization under uncertainty. First, uncertainty data are often collected from a wide spectrum of conditions, which are indicated by categorical labels. For example, uncertain power generation data of a solar farm are collected under different weather conditions, such as cloudy, sunny and rainy.³⁶ The occurrence probability of each weather condition is known in the data collection process, and typically embedded in the datasets. Moreover, the uncertainty data with the same label might not follow any commonly known distributions, and are often contaminated by

anomalous measurements. Therefore, a major research challenge is how to systematically and automatically handle labeled multi-class uncertainty data by leveraging the label information in the data-driven optimization framework. Second, we are confronted with the challenge of how to integrate different approaches for optimization under uncertainty in a holistic framework to leverage their respective advantages. The third challenge is to develop an efficient computational algorithm for the resulting large-scale multi-level optimization problem, which cannot be solved directly by any off-the-shelf optimization solvers.

This paper proposes a novel data-driven nested stochastic robust optimization (DDNSRO) framework that systematically and automatically handles labeled multi-class uncertainty data. In large datasets, uncertainty data are often attached with labels to indicate their data classes.³¹ For the labeled multi-class uncertainty data, we propose a data-driven uncertainty modeling process that includes two parts, i.e. probability distribution estimation for different data classes, and uncertainty set construction for high-dimensional uncertainty. The probability distribution for data classes is learned from uncertainty data through maximum likelihood estimation for the multinoulli distribution.^{37,38} To capture the nature of uncertainty data with different labels, a group of Dirichlet process mixture models is employed to model uncertainty with a variational inference algorithm.^{39,40} Since the Dirichlet process mixture model is Bayesian nonparametric, it allows automatic adjustment of its model complexity based on the data structure and complexity. Consequently, few presumptions about uncertain parameters, such as independence or symmetry, are required. Multiple basic uncertainty sets, instead of one, are unified to provide a high-fidelity description of uncertainties. These two pieces of uncertainty information are incorporated into the DDNSRO framework through a bi-level optimization structure. Two-stage stochastic programming is nested in the outer problem to optimize the expected objective over categorical data classes; robust optimization is nested as the inner problem to hedge against high-dimensional uncertainty and ensure computational tractability. Estimating a categorical distribution is much more computationally tractable than estimating a joint probability distribution of a high-dimensional uncertainty.³⁸ Therefore, the outer problem follows a two-stage stochastic programming structure to take advantage of the available probability information on data classes. Robust optimization, which uses an uncertainty set instead of accurate knowledge on probability distributions, is more suitable to be nested as the inner problem to tackle high-dimensional uncertainties. The DDNSRO problem is formulated as a multi-level mixed-integer linear program

(MILP). We further develop a tailored column-and-constraint generation (C&CG) algorithm to efficiently solve the resulting multi-level MILP problem, which cannot be solved directly by any off-the-shelf optimization solvers. To demonstrate the advantages of the proposed framework and the efficiency of the computational algorithm, a numerical example and two case studies on strategic planning of process networks under uncertainty are presented.

The major contributions of this paper are summarized as follows.

- A novel data-driven uncertainty modeling framework that systematically and automatically handles labeled multi-class uncertainty data;
- A general DDNSRO framework that organically integrates uncertainty data information and a state-of-the-art approach for optimization under uncertainty;
- A tailored C&CG algorithm that efficiently solves the resulting multi-level MILP problems;
- A large-scale application on process network planning under uncertainty.

The rest of this paper is organized as follows. The next section presents the general DDNSRO framework, which includes uncertainty modeling, optimization model and computational algorithm. It is followed by a numerical example and an application on process network planning under uncertainty. A conclusion is drawn at the end.

Data-Driven Nested Stochastic Robust Optimization Framework

In this section, we first provide a brief introduction to nested stochastic robust optimization. The proposed data-driven uncertainty model and the DDNSRO framework are presented next. A decomposition-based solution algorithm is further developed to efficiently solve the resulting multi-level optimization problem. Although the proposed DDNSRO framework might be applicable to some nonlinear optimization cases, we restrict the scope of this paper to the case of data-driven nested stochastic robust MILP under uncertainty to facilitate the presentation.

Nested stochastic robust optimization

Nested stochastic robust optimization framework combines two-stage stochastic programming and adaptive robust optimization (ARO).²⁹ In this subsection, we first analyze the strengths and weaknesses of two-stage stochastic programming and two-stage ARO. They are then

integrated in a novel form to leverage their corresponding advantages and complement respective shortcomings.

A general two-stage stochastic MILP in its compact form is given as follows.⁶

$$\begin{aligned} \min_{\mathbf{x}} \quad & \mathbf{c}^T \mathbf{x} + \mathbb{E}_{\mathbf{u}} [Q(\mathbf{x}, \mathbf{u})] \\ \text{s.t.} \quad & \mathbf{A}\mathbf{x} \geq \mathbf{d} \\ & \mathbf{x} \in R_+^{n_1} \times Z^{n_2} \end{aligned} \quad (1)$$

The recourse function $Q(\mathbf{x}, \mathbf{u})$ is defined as follows.

$$\begin{aligned} Q(\mathbf{x}, \mathbf{u}) = \min_{\mathbf{y}} \quad & \mathbf{b}^T \mathbf{y} \\ \text{s.t.} \quad & \mathbf{W}\mathbf{y} \geq \mathbf{h} - \mathbf{T}\mathbf{x} - \mathbf{M}\mathbf{u} \\ & \mathbf{y} \in R_+^{n_3} \end{aligned} \quad (2)$$

where \mathbf{x} is first-stage decisions made “here-and-now” before the uncertainty \mathbf{u} is realized, while the second-stage decisions or recourse decisions \mathbf{y} are postponed in a “wait-and-see” manner after the uncertainties are revealed. \mathbf{x} can include both continuous and integer variables, while \mathbf{y} only includes continuous variables.

Two-stage stochastic programming makes full use of probability distribution information, and aims to find a solution that performs well on average under all scenarios. However, an accurate joint probability distribution of high-dimensional uncertainty \mathbf{u} is required to calculate the expectation term in (1). Besides, the resulting two-stage stochastic programming problem could become computationally challenging as the number of scenarios increases.²¹

Another popular approach for optimization under uncertainty is ARO, which hedges against the worst-case uncertainty realization within an uncertainty set. A general two-stage ARO problem in its compact form is given as follows.^{41,42}

$$\begin{aligned} \min_{\mathbf{x}} \quad & \mathbf{c}^T \mathbf{x} + \max_{\mathbf{u} \in U} \min_{\mathbf{y} \in \Omega(\mathbf{x}, \mathbf{u})} \mathbf{b}^T \mathbf{y} \\ \text{s.t.} \quad & \mathbf{A}\mathbf{x} \geq \mathbf{d}, \quad \mathbf{x} \in R_+^{n_1} \times Z^{n_2} \\ & \Omega(\mathbf{x}, \mathbf{u}) = \{ \mathbf{y} \in R_+^{n_3} : \mathbf{W}\mathbf{y} \geq \mathbf{h} - \mathbf{T}\mathbf{x} - \mathbf{M}\mathbf{u} \} \end{aligned} \quad (3)$$

where \mathbf{x} is the vector of first-stage decision variables, and \mathbf{y} represents the vector of second-stage decisions. Note that \mathbf{x} includes both continuous and integer variables, and \mathbf{y} is the vector of continuous recourse variables. The first-stage decisions are made “here-and-now” prior to the resolution of uncertainty \mathbf{u} , and the second-stage decisions are adjustable to uncertainty realizations in a “wait-and-see” mode. U is an uncertainty set that characterizes the region in which

uncertainty realization resides. Note that the two-stage ARO problem in (3) is a tri-level optimization problem.

Existing ARO methods typically assume the uncertainty set U is given and known a priori, rather than constructing it directly from uncertainty data.³⁴ Robust optimization does not leverage available probability distribution information that could be extracted from uncertainty data. Moreover, they handle the uncertainty realizations as a whole, because the inner maximization problem over \mathbf{u} is not capable to differentiate the mixed uncertainty data with different labels and handle them separately. Consequently, the resulting solution can be overly conservative.

The nested stochastic robust optimization framework was recently proposed to organically integrate the two-stage stochastic programming approach with the ARO method. A general form of the nested stochastic robust MILP is given by,²⁹

$$\begin{aligned}
& \min_{\mathbf{x}} \mathbf{c}^T \mathbf{x} + \mathbb{E}_{\sigma \in \Pi} [\bar{C}_\sigma(\mathbf{x})] \\
& \text{s.t.} \quad \mathbf{Ax} \geq \mathbf{d} \\
& \quad \mathbf{x} \in R_+^{n_1} \times Z^{n_2} \\
& \left. \begin{aligned}
& \bar{C}_\sigma(\mathbf{x}) = \max_{\mathbf{u} \in U_\sigma} \min_{\mathbf{y}_\sigma} \mathbf{b}^T \mathbf{y}_\sigma \\
& \text{s.t.} \quad \mathbf{Wy}_\sigma \geq \mathbf{h} - \mathbf{T}\mathbf{x} - \mathbf{M}\mathbf{u} \\
& \quad \mathbf{y}_\sigma \in R_+^{n_3}
\end{aligned} \right\}, \forall \sigma \in \Pi
\end{aligned} \tag{4}$$

where σ is an uncertain scenario that influences the uncertainty set, and Π is a set of the scenarios. Two-stage stochastic programming approach is nested in the outer problem to optimize the expectation of objectives for different scenarios, and robust optimization is nested inside to hedge against the worst-case uncertainty realization. Instead of handling uncertainties in a “one-size-fits-all” manner, nested stochastic robust optimization could well address different types of uncertainties in a holistic framework.

The nested stochastic robust optimization method typically assumes the uncertainty probability distributions and uncertainty sets are given and known a priori, rather than connecting them directly with the uncertainty data. This assumption limits its application to the cases that uncertainty data are available, since the predefined probability distribution and manually constructed uncertainty sets might not accurately capture all necessary and sufficient information from the available uncertainty data. Thus, we propose a novel data-driven uncertainty modeling

framework for nested stochastic robust optimization with labeled multi-class uncertainty data to fill this knowledge gap.

Data-driven uncertainty modeling

In this subsection, we propose a data-driven uncertainty modeling framework that includes two parts, i.e. probability distribution estimation for different data classes, and uncertainty set construction from uncertainty data of the same data class. For the first part, the probability distribution for data classes is learned from the label information in mixed uncertainty data through maximum likelihood estimation. For the second part, a group of Dirichlet process mixture models is employed to construct uncertainty sets with a variational inference algorithm.

We consider the multi-class uncertainty data with labels $\{\mathbf{u}^{(i)}, c^{(i)}\}_{i=1}^L$, where $\mathbf{u}^{(i)}$ is i th uncertainty data point, $c^{(i)}$ is its corresponding label, and L is the total number of uncertainty data. Although the labeled uncertainty data is of practical relevance,³¹ existing literature on data-driven optimization under uncertainty are restricted to unlabeled uncertainty data $\{\mathbf{u}^{(i)}\}_{i=1}^L$.^{32,34}

The uncertainty information on the probability of different data classes can be extracted from mixed uncertainty data by leveraging their label information. The occurrence probabilities of data classes are modeled with a multinoulli distribution. The probability of each data class can be calculated through maximum likelihood estimation, as shown in (5).^{37,38}

$$p_s = \frac{\sum_i \mathbb{I}(c^{(i)} = s)}{L} \quad (5)$$

where p_s represents the occurrence probability of data class s , $c^{(i)}$ is the label associated with the i th uncertainty data point, $c^{(i)}=s$ indicates that the i th uncertainty data point is from data class s , and the indicator function is defined as follows.

$$\mathbb{I}(c^{(i)} = s) = \begin{cases} 1 & \text{if } c^{(i)} = s \\ 0 & \text{else} \end{cases} \quad (6)$$

As will be shown in the next subsection, the extracted probability distribution information for different data classes is incorporated into the two-stage stochastic programming framework nested as the outer optimization problem of DDNSRO.

The second part of the uncertainty modeling is the construction of data-driven uncertainty sets for uncertainty data in the same data class. The information on uncertainty sets is incorporated into the robust optimization nested as the inner optimization problem of DDNSRO. To handle the mixed uncertainty data, a group of Dirichlet process mixture models is employed, and uncertainty data with the same label are modeled using one separate Dirichlet process mixture model. The Dirichlet process mixture model is a powerful nonparametric Bayesian statistical model, which has an infinite-dimensional parameter space. Therefore, the resulting data-driven uncertainty set could adjust its complexity based on the data structure and complexity.

The Dirichlet process is defined as follows.⁴³ A random distribution F is said to be distributed as a Dirichlet process, denoted as $F \sim DP(\alpha, F_0)$, if for any fixed number of partitions $(\Theta_1, \dots, \Theta_r)$ of Θ , $(F(\Theta_1), \dots, F(\Theta_r))$ obeys a Dirichlet distribution, i.e.,

$$(F(\Theta_1), \dots, F(\Theta_r)) \sim Dir(\alpha F_0(\Theta_1), \dots, \alpha F_0(\Theta_r)) \quad (7)$$

where F_0 is a base distribution on Θ , α is the concentration parameter that indicates the users' belief in F_0 . Dir is the notation for the Dirichlet distribution. Besides, a random draw from the Dirichlet process has the following representation based on a stick-breaking construction.⁴⁴

$$F = \sum_{k=1}^{\infty} \pi_k \delta_{\theta_k} \quad (8)$$

where the weight $\pi_k = \beta_k \prod_{j=1}^{k-1} (1 - \beta_j)$, and β_k is the proportion of stick being broken from the remaining stick. β_k follows a Beta distribution, denoted as $\beta_k \sim \text{Beta}(1, \alpha)$. The random variable drawn from the base distribution F_0 is denoted as θ_k . δ_{θ_k} is a delta function which is equal to 1 at θ_k , and 0 otherwise.

The Dirichlet process is a distribution on distributions. A random draw from a Dirichlet process, i.e. $DP(\alpha, F_0)$, is a distribution F . We can still have a random draw from the distribution F . The Dirichlet process mixture model adds one more level to this hierarchy. It utilizes θ_k as the parameters of the data distribution. As shown in eq. (8), the Dirichlet process mixture model can be interpreted as a mixture model that has a potentially infinite number of mixture components. The general Dirichlet process mixture model is summarized as follows.⁴⁵

$$\begin{aligned}
\beta_k | \alpha &\sim \text{Beta}(1, \alpha) \\
\theta_k | F_0 &\sim F_0 \\
l_i | \{\beta_1, \beta_2, \dots\} &\sim \text{Mult}(\pi(\beta)) \\
o_i | l_i &\sim p(o_i | \theta_{l_i})
\end{aligned} \tag{9}$$

where *Mult* denotes a multinomial distribution, and l_i is the index of mixture components to which the observation o_i is assigned.

Variational inference algorithm is employed for the Dirichlet process mixture model.^{45,46} In Bayesian statistics, the model parameters are considered as random variables, and the goal of inference is to obtain the posterior distribution of these latent random variables. The mixtures of Gaussian distributions are adopted in this work. $\theta_k = (\boldsymbol{\eta}_k, \mathbf{H}_k)$ includes mean vector and precision matrix. It is assumed that $\theta_k \sim \text{NW}(\boldsymbol{\mu}_k, \lambda_k, \omega_k, \boldsymbol{\Psi}_k)$, where *NW* represents the normal Wishart distribution. According to the variational inference algorithm, the posterior distribution is approximated by a factorized variational distribution $q(\mathbf{l}, \boldsymbol{\beta}, \alpha, \boldsymbol{\eta}, \mathbf{H})$, given by,

$$q(\mathbf{l}, \boldsymbol{\beta}, \alpha, \boldsymbol{\eta}, \mathbf{H}) = \prod_{i=1}^N q(l_i) \prod_{k=1}^{M-1} q(\beta_k) q(\alpha) \prod_{k=1}^M q(\boldsymbol{\eta}_k, \mathbf{H}_k) \tag{10}$$

where M is the truncation level.

Based on the extracted information, we propose a data-driven nonparametric uncertainty set for data class s using both l_1 and l_∞ norms in (11) and (12).³⁴

$$U_s = \bigcup_{i: \gamma_{s,i} \geq \gamma^*} U_{s,i} = U_{s,1} \bigcup U_{s,2} \cdots \bigcup U_{s,m(s)} \tag{11}$$

$$U_{s,i} = \left\{ \mathbf{u} \mid \mathbf{u} = \boldsymbol{\mu}_{s,i} + \kappa_{s,i} \boldsymbol{\Psi}_{s,i}^{1/2} \Lambda_{s,i} \mathbf{z}, \|\mathbf{z}\|_\infty \leq 1, \|\mathbf{z}\|_1 \leq \Phi_{s,i} \right\} \tag{12}$$

where U_s is the data-driven uncertainty set for data class s , $U_{s,i}$ is the basic uncertainty set corresponding to the i th component for data class s , $\Lambda_{s,i}$ is a scaling factor, $\gamma_{s,i}$ is the weight of the

i th mixture component for data class s , $\gamma_{s,i} = \frac{\tau_{s,i}}{\tau_{s,i} + \nu_{s,i}} \prod_{j=1}^{i-1} \frac{\nu_{s,j}}{\tau_{s,j} + \nu_{s,j}}$ and $\gamma_{s,M} = 1 - \sum_{i=1}^{M-1} \gamma_{s,i}$. The

weight $\gamma_{s,i}$ indicates the probability of the corresponding mixture component. γ^* is a threshold value with a typical value of 2% or 5%. $m(s)$ is a total number of mixture components for data class s .

$\kappa_{s,i} = \sqrt{\frac{\lambda_{s,i} + 1}{\lambda_{s,i} (\omega_{s,i} + 1 - \dim(\mathbf{u}))}}$,³⁹ and $\tau_{s,i}$, $\nu_{s,i}$, $\boldsymbol{\mu}_{s,i}$, $\lambda_{s,i}$, $\omega_{s,i}$, $\boldsymbol{\Psi}_{s,i}$ are the inference results of the i th

component learned from uncertainty data of data class s . The details of the variational inference algorithm is provided in Appendix A. The uncertainty set U_s is a union of several basic uncertainty

sets $U_{s,i}$. The basic uncertainty set $U_{s,i}$ can be considered as a data-driven version of the budget based uncertainty set,²⁵ and $\Phi_{s,i}$ is its uncertainty budget, which controls the size of the uncertainty set.

The proposed data-driven uncertainty set is referred to as “nonparametric” because the number of its parameters grows as the structure of uncertain data becomes more complex. Although the representation capability of each component is limited, a mixture of components is capable to capture more complex characteristics embedded within uncertainty data in each data class. Therefore, multiple basic uncertainty sets, instead of one, are unified to capture the nature of uncertainty data accurately. It is worth noting that the number of basic uncertainty sets $m(s)$ for each data class might be different, and this number is adjustable to the complexity of uncertainty data automatically, as will be illustrated in Numerical Example section.

The proposed data-driven uncertainty modeling approach combines probability distribution estimation for different data classes with uncertainty set construction for the high-dimensional uncertainty. A novel DDNSRO approach is further proposed by organically integrating this data-driven uncertainty model with the nested stochastic robust optimization framework.

Data-driven nested stochastic robust optimization model

Based on the uncertainty information, DDNSRO framework is proposed to organically integrate uncertainty data information with the nested stochastic robust optimization framework, as shown in (13).

$$\begin{aligned}
& \min_{\mathbf{x}} \mathbf{c}^T \mathbf{x} + \mathbb{E}_{s \in \Xi} \left[\max_{\mathbf{u} \in U_{s,1} \cup U_{s,2} \dots \cup U_{s,m(s)}} \min_{\mathbf{y}_s \in \Omega(\mathbf{x}, \mathbf{u})} \mathbf{b}^T \mathbf{y}_s \right] \\
& \text{s.t. } \mathbf{A}\mathbf{x} \geq \mathbf{d}, \quad \mathbf{x} \in R_+^{n_1} \times Z^{n_2} \\
& U_{s,i} = \left\{ \mathbf{u} \mid \mathbf{u} = \boldsymbol{\mu}_{s,i} + \kappa_{s,i} \boldsymbol{\Psi}_{s,i}^{1/2} \boldsymbol{\Lambda}_{s,i} \mathbf{z}, \quad \|\mathbf{z}\|_{\infty} \leq 1, \quad \|\mathbf{z}\|_1 \leq \Phi_{s,i} \right\} \\
& \Omega(\mathbf{x}, \mathbf{u}) = \left\{ \mathbf{y}_s \in R_+^{n_3} : \mathbf{W}\mathbf{y}_s \geq \mathbf{h} - \mathbf{T}\mathbf{x} - \mathbf{M}\mathbf{u} \right\}
\end{aligned} \tag{13}$$

where $\Xi = \{1, 2, \dots, C\}$ is the set of data classes, C is the total number of data classes, $m(s)$ is a total number of mixture components for data class s . Each data class corresponds to a scenario in the two-stage stochastic program nested outside the DDNSRO framework. Therefore, a data class corresponds to a scenario in the DDNSRO framework. It is worth noting that the DDNSRO problem in (13) is a multi-level MILP that involves mixed-integer first-stage decisions, and continuous recourse decisions.

In the DDNSRO framework, the outer optimization problem follows a two-stage stochastic programming structure, and robust optimization is nested as the inner optimization problem to handle high-dimensional uncertainty \mathbf{u} . DDNSRO aims to find a solution that performs well on average across all data classes by making full use of their occurrence probabilities. Instead of treating all the uncertainty data as a whole, we explicitly account for uncertainty data with different labels in the DDNSRO framework. Nested stochastic robust optimization structure is employed because it is more suitable to handle different types of uncertainties in a holistic framework. Note that DDNSRO is a general framework for data-driven optimization under uncertainty, while existing nested stochastic robust optimization methods assume uncertainty information is given *a priori* rather than learning it from uncertainty data.

There are two reasons that two-stage stochastic programming is nested as the outer optimization problem while robust optimization is nested as the inner optimization problem. First, the proposed DDNSRO framework aims to balance all data classes instead of focusing only on the worst-case data class, and it also ensures the robustness of the solution. Second, estimating the probability distribution for data classes accurately is much more computationally tractable than for the high-dimensional continuous uncertainty.³⁸ Consequently, it is better to employ uncertainty set to characterize high-dimensional uncertain parameters in the inner optimization problem. On the other hand, stochastic programming is more suitable as the outer optimization problem to leverage the probability information of data classes.

Note that the proposed data-driven uncertainty set for each data class in (11) is a union of several basic uncertainty sets. Therefore, we reformulate the DDNSRO model in (13) into (14), as given below.

$$\begin{aligned}
& \min_{\mathbf{x}} \mathbf{c}^T \mathbf{x} + \mathbb{E}_{s \in \Xi} \left[\max_{i \in \{1, \dots, m(s)\}} \max_{\mathbf{u} \in U_{s,i}} \min_{\mathbf{y}_s \in \Omega(\mathbf{x}, \mathbf{u})} \mathbf{b}^T \mathbf{y}_s \right] \\
& \text{s.t. } \mathbf{A}\mathbf{x} \geq \mathbf{d}, \quad \mathbf{x} \in R_+^{n_1} \times Z^{n_2} \\
& \quad U_{s,i} = \left\{ \mathbf{u} \mid \mathbf{u} = \boldsymbol{\mu}_{s,i} + \kappa_{s,i} \boldsymbol{\Psi}_{s,i}^{1/2} \boldsymbol{\Lambda}_{s,i} \mathbf{z}, \quad \|\mathbf{z}\|_{\infty} \leq 1, \quad \|\mathbf{z}\|_1 \leq \Phi_{s,i} \right\} \\
& \quad \Omega(\mathbf{x}, \mathbf{u}) = \left\{ \mathbf{y}_s \in R_+^{n_3} : \mathbf{W}\mathbf{y}_s \geq \mathbf{h} - \mathbf{T}\mathbf{x} - \mathbf{M}\mathbf{u} \right\}
\end{aligned} \tag{14}$$

Due to the finite number of data classes, the model in (14) is further reformulated with the occurrence probability for each data class as shown in (15).

$$\begin{aligned}
& \min_{\mathbf{x}} \mathbf{c}^\top \mathbf{x} + \sum_{s \in \Xi} p_s \cdot \left(\max_{i \in \{1, \dots, m(s)\}} \max_{\mathbf{u} \in U_{s,i}} \min_{\mathbf{y}_s \in \Omega(\mathbf{x}, \mathbf{u})} \mathbf{b}^\top \mathbf{y}_s \right) \\
& \text{s.t. } \mathbf{Ax} \geq \mathbf{d}, \quad \mathbf{x} \in R_+^{n_1} \times Z^{n_2} \\
& U_{s,i} = \left\{ \mathbf{u} \mid \mathbf{u} = \boldsymbol{\mu}_{s,i} + \kappa_{s,i} \boldsymbol{\Psi}_{s,i}^{1/2} \boldsymbol{\Lambda}_{s,i} \mathbf{z}, \quad \|\mathbf{z}\|_\infty \leq 1, \quad \|\mathbf{z}\|_1 \leq \Phi_{s,i} \right\} \\
& \Omega(\mathbf{x}, \mathbf{u}) = \left\{ \mathbf{y}_s \in R_+^{n_3} : \mathbf{W}\mathbf{y}_s \geq \mathbf{h} - \mathbf{T}\mathbf{x} - \mathbf{M}\mathbf{u} \right\}
\end{aligned} \tag{15}$$

where p_s represents the occurrence probability of data class s , and can be calculated by (5). Note that the uncertainty information extracted from data, including data-driven uncertainty sets and probability distributions of data classes, is seamlessly integrated into the optimization model in (15).

The DDNSRO model explicitly accounts for the label information within multi-class uncertainty data, and balance different data classes by using the weighted sum based on their occurrence probabilities. Robust optimization is nested as the inner optimization problem to handle high-dimensional uncertainty \mathbf{u} , thus providing a good balance between solution quality and computational tractability. Moreover, multiple basic uncertainty sets $U_{s,i}$ are unified to handle the data complexity (such as correlation, asymmetry and multimode), and this approach leads to the inner max-max optimization problem in (15). An overview of the proposed DDNSRO framework for labeled multi-class uncertainty data is shown in Figure 1. Uncertainty data are depicted using circles with different colors to indicate its associated data class, and they are treated separately using a group of Dirichlet process mixture models. The probability distribution of data classes can be obtained from uncertainty data using eq. (5). As can be observed, the proposed framework, which leverages the strengths of stochastic programming and robust optimization, unlocks the value of labeled multi-class uncertainty data.

The resulting DDNSRO problem is a multi-level MILP problem. Due to the multi-level structure, it cannot be solved directly by any off-the-shelf optimization solvers. To this end, an efficient computational algorithm is further proposed in the next subsection to address this computational challenge.

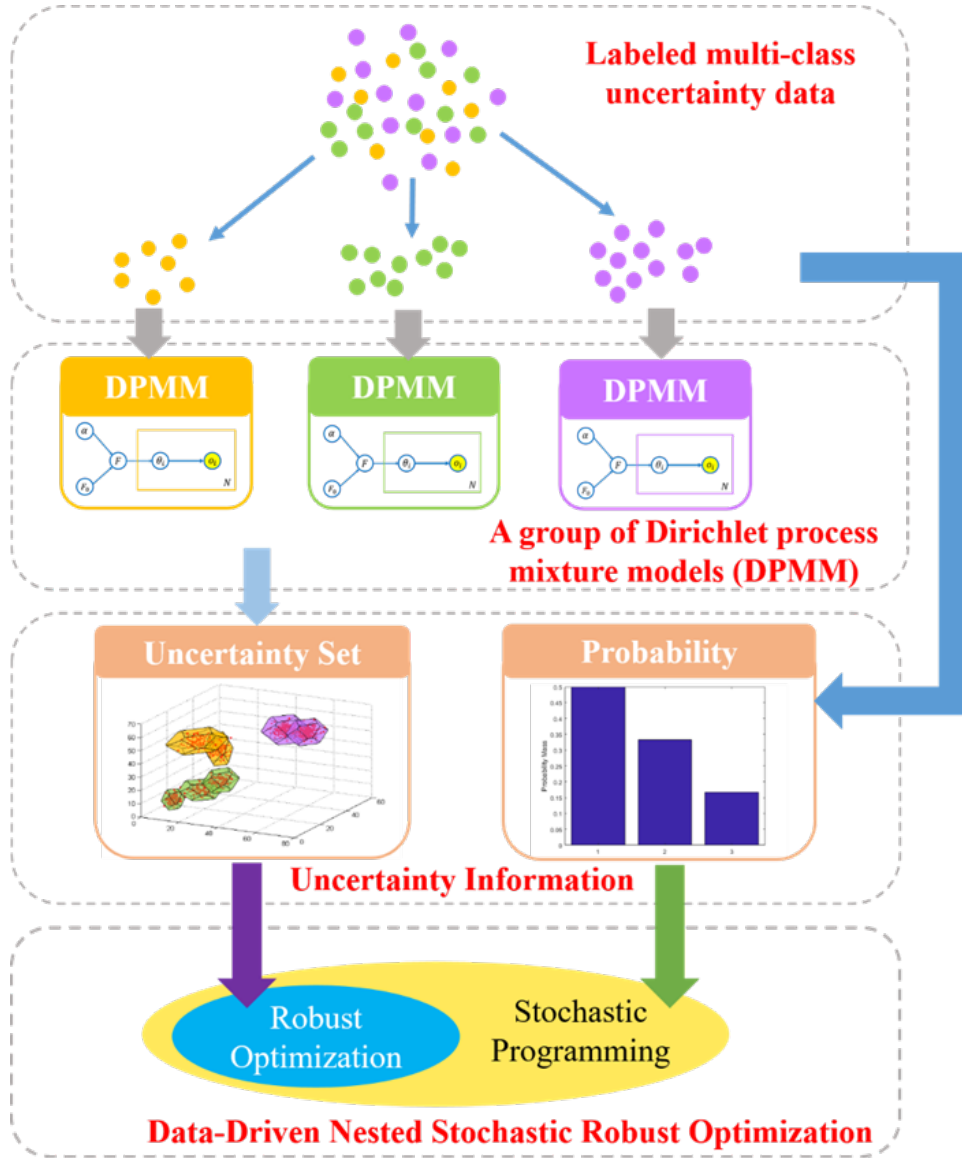


Figure 1. The proposed DDNSRO framework that handles labeled multi-class uncertainty data.

The tailored column-and-constraint generation algorithm

In this section, we address computational challenge of solving the multi-level DDNSRO problem by proposing a decomposition-based solution algorithm. This algorithm is designed in the line of the C&CG algorithm.⁴² We first decompose the multi-level MILP shown in (15) into a master problem and many groups of sub-problems, where each group corresponds to a data class. Moreover, there are a number of sub-problems in each group, and each sub-problem corresponds to a component in the Dirichlet process mixture model.

First, the multi-level optimization problem can be reformulated to an equivalent single-level optimization problem.⁴⁷ Having observed that the uncertainties at their optimal solution will be one extreme point of a basic uncertainty set, we enumerate all the extreme points, and introduce their corresponding recourse variables to transform the original multi-level problem into a single-level full master problem. However, this single-level optimization problem could be a large-scale optimization problem due to the potentially large number of extreme points. Therefore, we partially enumerate the extreme points, and construct the master problem. Because the master problem **(MP)** contains only a subset of the extreme points, it provides a relaxation of the original problem. The master problem **(MP)** is shown below.

$$\begin{aligned}
(\text{MP}) \quad & \min_{\mathbf{x}, \eta, \mathbf{y}_s^l} \mathbf{c}^\top \mathbf{x} + \eta \\
& \text{s.t. } \mathbf{Ax} \geq \mathbf{d} \\
& \eta \geq \sum_s p_s (\mathbf{b}^\top \mathbf{y}_s^l), \quad l=1, \dots, r \\
& \mathbf{T}\mathbf{x} + \mathbf{W}\mathbf{y}_s^l \geq \mathbf{h} - \mathbf{M}\mathbf{u}_s^l, \quad l=1, \dots, r, \forall s \\
& \mathbf{x} \in \mathbb{R}_+^{n_1} \times Z^{n_2}, \quad \mathbf{y}_s^l \in \mathbb{R}_+^{n_3}, \quad l=1, \dots, r, \forall s
\end{aligned}$$

where s is the index for data class, and \mathbf{u}_s^l is the enumerated uncertainty realization at the l th iteration for data class s , \mathbf{y}_s^l is its corresponding recourse variable, r stands for the current number of iterations.

To enumerate the important uncertainty realization on-the-fly, the sub-problem in (16) is solved in each iteration.

$$\begin{aligned}
Q_{s,i}(\mathbf{x}) &= \max_{\mathbf{u} \in U_{s,i}} \min_{\mathbf{y}_s} \mathbf{b}^\top \mathbf{y}_s \\
& \text{s.t. } \mathbf{W}\mathbf{y}_s \geq \mathbf{h} - \mathbf{T}\mathbf{x} - \mathbf{M}\mathbf{u} \\
& \mathbf{y}_s \in \mathbb{R}_+^{n_3}
\end{aligned} \tag{16}$$

It is worth noting that (16) is a max-min optimization problem, which can be transformed to a single-level optimization problem by employing strong duality or KKT conditions. To make the sub-problem computationally tractable, we dualize the inner optimization problem of (16), which is a linear program with regard to \mathbf{y}_s , and merge the dual problem with the maximization problem with respect to \mathbf{u} . The resulting problem is shown in (17).

$$\begin{aligned}
Q_{s,i}(\mathbf{x}) &= \max_{\mathbf{z}, \boldsymbol{\varphi}} (\mathbf{h} - \mathbf{T}\mathbf{x} - \mathbf{M}\boldsymbol{\mu}_{s,i})^T \boldsymbol{\varphi} - \sum_t \sum_j (\kappa_{s,i} \mathbf{M}\boldsymbol{\Psi}_{s,i}^{1/2} \Lambda_{s,i})_{tj} \mathbf{z}_j \boldsymbol{\varphi}_t \\
&\text{s.t. } \mathbf{W}^T \boldsymbol{\varphi} \leq \mathbf{b} \\
&\quad \boldsymbol{\varphi} \geq \mathbf{0} \\
&\quad \|\mathbf{z}\|_\infty \leq 1, \|\mathbf{z}\|_1 \leq \Phi_{s,i}
\end{aligned} \tag{17}$$

where $\boldsymbol{\varphi}$ is the vector of dual variables associated with the constraints $\mathbf{W}\mathbf{y} \geq \mathbf{h} - \mathbf{T}\mathbf{x} - \mathbf{M}\mathbf{u}$, $\boldsymbol{\varphi}_t$ represents the t th component in vector $\boldsymbol{\varphi}$, and \mathbf{z}_j is the j th component in vector \mathbf{z} .

Since there are bilinear terms $\mathbf{z}_j \boldsymbol{\varphi}_t$ in the objective of (17), we need to further reformulate the sub-problem in (17). To facilitate the derivation, \mathbf{z}_j can be divided into two parts $\mathbf{z}_j = \mathbf{z}_j^+ - \mathbf{z}_j^-$. Thus, we have

$$\mathbf{u} = \boldsymbol{\mu}_{s,i} + \kappa_{s,i} \boldsymbol{\Psi}_{s,i}^{1/2} \Lambda_{s,i} (\mathbf{z}^+ - \mathbf{z}^-) \tag{18}$$

Following the existing literature,^{48,49} the uncertainty budget parameter $\Phi_{s,i}$ is typically set as an integer value due to its physical meaning. For the integer uncertainty budget, the optimal \mathbf{z}_j^+ and \mathbf{z}_j^- take the values of 0 or 1, and these two variables can be restricted to binary variables. By using Glover's linearization for the bilinear terms $\mathbf{G}_{ij}^+ = \mathbf{z}_j^+ \boldsymbol{\varphi}_t$ and $\mathbf{G}_{ij}^- = \mathbf{z}_j^- \boldsymbol{\varphi}_t$,⁵⁰ which are the products of a binary variable \mathbf{z}_j^+ (and \mathbf{z}_j^-) and a continuous variable $\boldsymbol{\varphi}_t$, we can reformulate (17) to the following problem (SUP_{s,i}).

$$\begin{aligned}
Q_{s,i}(\mathbf{x}) &= \max_{\boldsymbol{\varphi}, \mathbf{z}^+, \mathbf{z}^-, \mathbf{G}^+, \mathbf{G}^-} (\mathbf{h} - \mathbf{T}\mathbf{x} - \mathbf{M}\boldsymbol{\mu}_{s,i})^T \boldsymbol{\varphi} - \text{Tr} \left((\kappa_{s,i} \mathbf{M}\boldsymbol{\Psi}_{s,i}^{1/2} \Lambda_{s,i})^T (\mathbf{G}^+ - \mathbf{G}^-) \right) \\
&\text{s.t. } \mathbf{W}^T \boldsymbol{\varphi} \leq \mathbf{b} \\
&\quad \boldsymbol{\varphi} \geq \mathbf{0} \\
&\quad \mathbf{0} \leq \mathbf{G}^+ \leq \boldsymbol{\varphi} \cdot \mathbf{e}^T \\
&\quad \mathbf{0} \leq \mathbf{G}^- \leq \boldsymbol{\varphi} \cdot \mathbf{e}^T \\
&\quad \mathbf{G}^+ \leq \tilde{\mathbf{e}} \cdot (M_0 \cdot \mathbf{z}^+)^T \\
&\quad \mathbf{G}^- \leq \tilde{\mathbf{e}} \cdot (M_0 \cdot \mathbf{z}^-)^T \\
&\quad \mathbf{G}^+ \geq \boldsymbol{\varphi} \cdot \mathbf{e}^T - \tilde{\mathbf{e}} \cdot (M_0 \cdot (\mathbf{e} - \mathbf{z}^+))^T \\
&\quad \mathbf{G}^- \geq \boldsymbol{\varphi} \cdot \mathbf{e}^T - \tilde{\mathbf{e}} \cdot (M_0 \cdot (\mathbf{e} - \mathbf{z}^-))^T \\
&\quad \mathbf{e}^T (\mathbf{z}^+ + \mathbf{z}^-) \leq \Phi_{s,i} \\
&\quad \mathbf{z}^+ + \mathbf{z}^- \leq \mathbf{e}, \quad \mathbf{z}^+, \mathbf{z}^- \in \{0, 1\}^K
\end{aligned} \tag{SUP_{s,i}}$$

\mathbf{e} and $\tilde{\mathbf{e}}$ both represent column vectors whose elements are all ones, but they have different dimensions, i.e., $\dim(\mathbf{e}) = \dim(\mathbf{u}) = K$ and $\dim(\tilde{\mathbf{e}}) = \dim(\boldsymbol{\varphi})$. The t th row and j th column elements of matrices \mathbf{G}^+ and \mathbf{G}^- are \mathbf{G}_{ij}^+ and \mathbf{G}_{ij}^- , respectively. The notation Tr denotes the trace of a matrix, e.g. for matrix $\mathbf{Q} = [q_{ij}] \in R^{n \times n}$, $\text{Tr}(\mathbf{Q}) = \sum_{i=1}^n q_{ii}$. Note that the vector or matrix inequalities should be interpreted elementwise.

The proposed solution algorithm iteratively solves a sequence of master problems and sub-problems until the relative optimality gap reduces to a predefined tolerance. The pseudocode of the algorithm is given in Figure 2, where ζ denotes the predefined tolerance, and C represents the total number of data classes. As the optimality and feasibility cuts are added to the master problem in each iteration, the lower bound provided by **(MP)** becomes tighter as the iteration moves on. Since the total number of extreme points is finite, the algorithm terminates within finite iterations.

Algorithm. The proposed tailored C&CG algorithm

```

1:   Set  $LB \leftarrow -\infty$ ,  $UB \leftarrow +\infty$ ,  $k \leftarrow 0$ , and  $\zeta$ ;
2:   while  $\left| \frac{UB-LB}{UB} \right| > \zeta$  do
3:       Solve (MP) to obtain  $\mathbf{x}_{k+1}^*$ ,  $\eta_{k+1}^*$ ,  $\mathbf{y}_s^{1*}, \dots, \mathbf{y}_s^{k*}$ ;
4:       Update  $LB \leftarrow \mathbf{c}^T \mathbf{x}_{k+1}^* + \eta_{k+1}^*$ ;
5:       for  $s=1$  to  $C$  do
6:           for  $i=1$  to  $m(s)$  do
7:               Solve (16) to obtain  $\mathbf{u}_{s,i}^{k+1}$  and  $Q_{s,i}(\mathbf{x}_{k+1}^*)$ ;
8:           end
9:            $i^* \leftarrow \arg \max_i Q_{s,i}(\mathbf{x}_{k+1}^*)$ ;
10:           $\mathbf{u}_s^{k+1} \leftarrow \mathbf{u}_{s,i^*}^{k+1}$  and  $Q_s(\mathbf{x}_{k+1}^*) \leftarrow Q_{s,i^*}(\mathbf{x}_{k+1}^*)$ ;
11:       end
12:       Update  $UB \leftarrow \min \left\{ UB, \mathbf{c}^T \mathbf{x}_{k+1}^* + \sum_{s=1} p_s \cdot Q_s(\mathbf{x}_{k+1}^*) \right\}$ ;
13:       Create second-stage variables  $\mathbf{y}_s^{k+1}$  and add cuts
14:        $\eta \geq \sum_s p_s (\mathbf{b}^T \mathbf{y}_s^{k+1})$  and  $\mathbf{T}\mathbf{x} + \mathbf{W}\mathbf{y}_s^{k+1} \geq \mathbf{h} - \mathbf{M}\mathbf{u}_s^{k+1}$  to (MP);
15:        $k \leftarrow k + 1$ ;
16:   end
17:   return  $UB$ ;

```

Figure 2. The pseudocode of the proposed computational algorithm.

Relationship with the existing data-driven adaptive nested robust optimization framework

In this subsection, we discuss the relationship between the DDNSRO framework proposed in this work and the recently proposed data-driven adaptive nested robust optimization (DDANRO) framework reported in our earlier publication.³⁴

The DDANRO framework in its general form has a four-level optimization structure, as given below.

$$\begin{aligned}
& \min_{\mathbf{x}} \mathbf{c}^\top \mathbf{x} + \max_{i \in \{1, \dots, m\}} \max_{\mathbf{u} \in U_i} \min_{\mathbf{y} \in \Omega(\mathbf{x}, \mathbf{u})} \mathbf{b}^\top \mathbf{y} \\
& \text{s.t. } \mathbf{Ax} \geq \mathbf{d}, \quad \mathbf{x} \in \mathbb{R}_+^{n_1} \times \mathbb{Z}^{n_2} \\
& U_i = \left\{ \mathbf{u} \mid \mathbf{u} = \boldsymbol{\mu}_i + \kappa_i \boldsymbol{\Psi}_i^{1/2} \Lambda_i \mathbf{z}, \quad \|\mathbf{z}\|_\infty \leq 1, \quad \|\mathbf{z}\|_1 \leq \Delta_i \right\} \\
& \Omega(\mathbf{x}, \mathbf{u}) = \left\{ \mathbf{y} \in \mathbb{R}_+^{n_3} : \mathbf{Wy} \geq \mathbf{h} - \mathbf{T}\mathbf{x} - \mathbf{M}\mathbf{u} \right\}
\end{aligned} \tag{19}$$

It is worth noting that the DDNSRO framework proposed in this paper could be considered as a generalization of the DDANRO framework, which handles uncertainty data homogeneously without considering the label information.³⁴ DDNSRO greatly enhances the capabilities of DDANRO, and expands its application scope to more complex uncertainty data structures. There are some similarities between DDNSRO and DDANRO. For example, they both employ data-driven uncertainty sets, and have multi-level optimization structures. Moreover, DDANRO can be considered as a special case of DDNSRO when there is only one class of uncertainty data. Specifically, if there is only one data class, we can simplify the weighted sum in (15) as a single term, and drop the index s in (15), such that the DDNSRO model shown in (15) reduces to the DDANRO model in (19). Thus, the DDANRO framework is more appropriate to handle single-class or unlabeled uncertainty data, while the proposed DDNSRO framework, on the other hand, is suitable for handling labeled multi-class uncertainty data systematically.

Numerical Example

In this section, a small numerical example of the proposed DDNSRO framework, as shown in (20), is presented to demonstrate its advantages over other methods for optimization under uncertainty.

We consider the following numerical example:

$$\begin{aligned}
& \min_{\mathbf{x}} 3x_1 + 5x_2 + 6x_3 + \mathbb{E}_{s \in \Xi} \left[\max_{\mathbf{u} \in U_s} \min_{\mathbf{y}} 6y_1 + 10y_2 + 12y_3 \right] \\
& \text{s.t. } x_1 + x_2 + x_3 \leq 200 \\
& \quad x_1 + y_1 \geq u_1 \\
& \quad x_2 + y_2 \geq u_2 \\
& \quad x_3 + y_3 \geq u_3 \\
& \quad x_i, y_i \geq 0, \quad i = 1, 2, 3
\end{aligned} \tag{20}$$

where x_1 , x_2 and x_3 are the first-stage or “here-and-now” decision variables, u_1 , u_2 and u_3 are the uncertain parameters, and y_1 , y_2 and y_3 are the second-stage or “wait-and-see” decision variables.

Note that the “here-and-now” decisions are made prior to the resolution of uncertainties, whereas “wait-and-see” decisions could be made after the uncertainties are revealed. The notation Ξ represents the set of data classes, and s is the corresponding element. The data-driven uncertainty set U_s is defined in (11).

The scatter plot of uncertainty data is shown in Figure 3, where the red points represent uncertainty realizations of u_1 , u_2 and u_3 . A total of 1,000 labeled uncertainty data points are used for uncertainty modeling in this case study. There are 4 labels within uncertainty data, which indicates that there are 4 data classes in total. Note that uncertainty data from different data classes are indicated with disparate shapes in Figure 3. Moreover, uncertainty data in the same data class could exhibit complex characteristics, such as correlation, asymmetry and multimode.

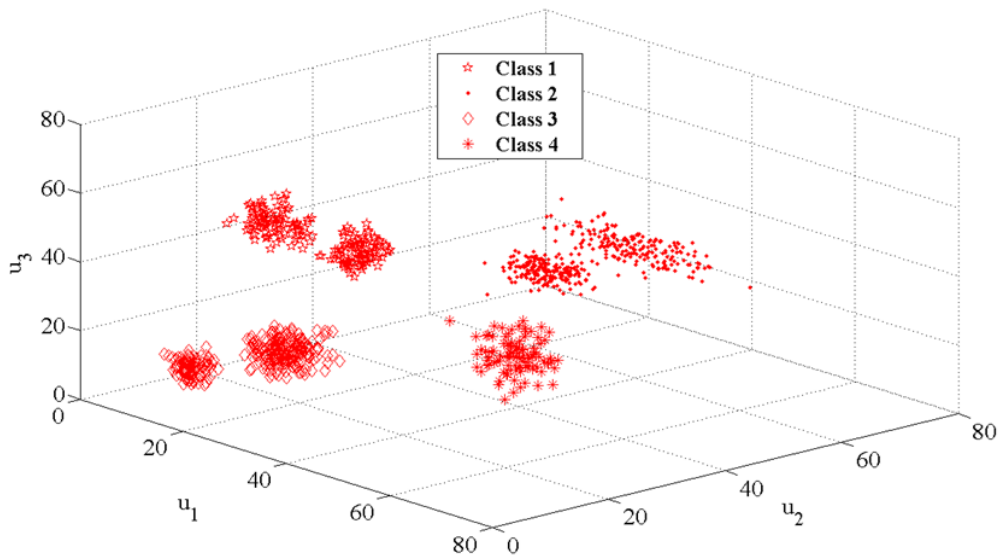


Figure 3. The scatter plot of uncertainty data in the numerical example.

Following the proposed data-driven uncertainty modeling framework, the occurrence probabilities of different data classes are inferred from the label information embedded within uncertainty data. The computational results show that the probabilities of data classes 1 - 4 are 0.2, 0.4, 0.3 and 0.1, respectively. Moreover, the uncertainty modeling results also show that there are two components in the Dirichlet process mixture models for data class 1-3, while there is only one component for data class 4. The occurrence probabilities of each data class are listed in Figure 4. The data-driven uncertainty sets with uncertainty budget $\Phi=1.8$ are also constructed for each data class, and are depicted using different colors shown in Figure 4. From Figure 4, we can see that

the distributional features of uncertainty data are automatically captured by the proposed data-driven uncertainty model. For example, the uncertainty set for data class 2 accurately captures the bimodal feature in uncertainty data, and the correlations among uncertain parameters u_1 , u_2 and u_3 . Besides, the beauty of the proposed data-driven uncertainty set is its automatic adjustment of complexity to that of data. As can be seen from Figure 3, the uncertainty data from data class 2 exhibit higher complexity than those from data class 4. Therefore, the proposed data-driven uncertainty set in dark green color for data class 2 automatically adjusts model complexity by increasing the number of basic uncertainty sets. Based on the data-driven uncertainty information in Figure 4, the resulting DDNSRO problem can be solved using the computational algorithm proposed in the previous section.

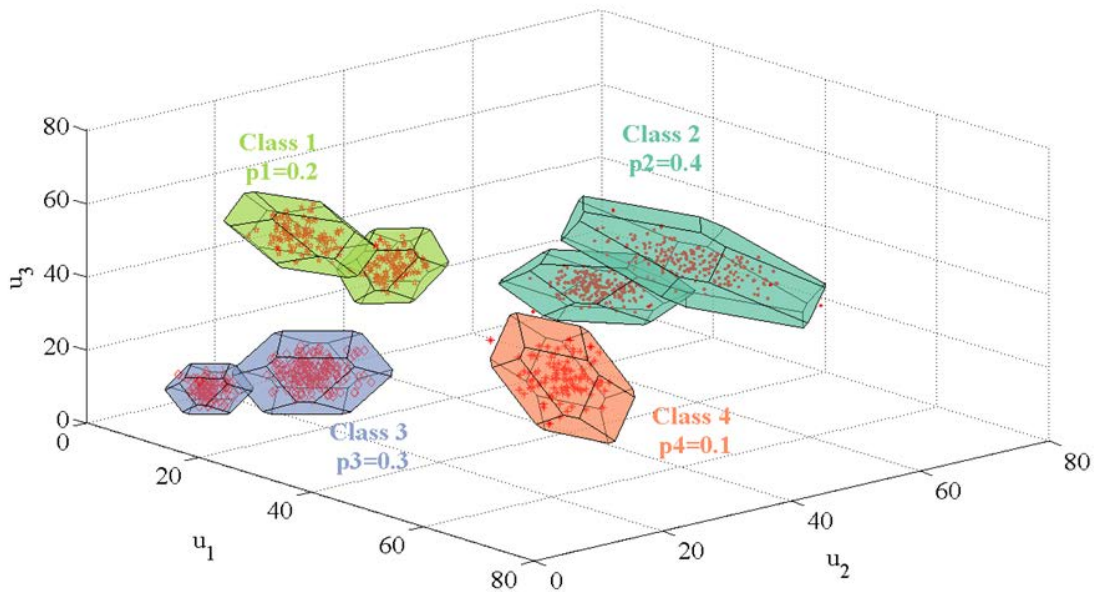


Figure 4. The data-driven uncertainty modeling results for the four data classes in the numerical example.

The computational experiments are implemented on a computer with an Intel (R) Core (TM) i7-6700 CPU @ 3.40 GHz and 32 GB RAM, and a Windows 10 64-bit operating system. The optimization models and the proposed tailored C&CG algorithm are coded in GAMS 24.7.3. We set the relative optimality gap for the proposed tailored C&CG algorithm to be 0.01%.

To demonstrate the superiority of the proposed approach, the deterministic optimization method, the two-stage ARO approach with a box set,²⁶ the two-stage stochastic programming

approach,⁶ and the DDANRO method are also implemented for comparisons. In the two-stage stochastic programming problem, each data point in Figure 3 corresponds to a scenario. There are 1,000 scenarios in total, and the probability of each scenario is given as 0.001. The resulting two-stage stochastic programming problem is solved using the multi-cut Benders decomposition algorithm.⁵¹ Note that the relative optimality gap for the multi-cut Benders decomposition algorithm is set as the same as that of the tailored C&CG algorithm to make a fair comparison. The numerical results are shown in Table 1. In the deterministic optimization method, the uncertain parameters are set to be their mean values of the uncertainty data. Although the deterministic approach achieves a low objective value in the minimization problem, its optimal solution could become infeasible when the parameters u_1 , u_2 and u_3 are subject to uncertainty. The two-stage stochastic programming approach focuses on the expected objective value, while the two-stage ARO and the DDANRO methods aim to minimize the worst-case objective value. Therefore, the objective value of the two-stage stochastic programming approach is lower than those of the robust optimization methods. Compared with the two-stage stochastic programming approach, the proposed DDNSRO approach is more computationally efficient (12s v.s. 477s). From Table 1, we can observe that the two-stage ARO and DDANRO methods tend to choose larger values for the solution of “here-and-now” decision variables, compared with the DDNSRO approach. The reason is that both the “here-and-now” decision x_i and the recourse decision y_i can be large enough to make the constraint $x_i + y_i \geq u_i$ feasible given the uncertainty parameter u_i . However, the second-stage decision variable y_i has a higher cost coefficient than that of the first-stage decision variable x_i . Therefore, the two-stage ARO and DDANRO methods, which hedge against the worst-case uncertainty realization among all 4 data classes, avoid taking the “expensive” recourse actions by enlarging their “here-and-now” decision variables.

Table 1. Results of different optimization methods in the numerical example.

	Deterministic optimization	Two-stage stochastic programming	Two-stage ARO	DDANRO $\Delta=1.8^*$	DDNSRO $\Phi=1.8^\#$
Min.obj.	455.3	646.4	964.0	944.6	795.4
Iterations	N/A	7	2	5	6
Total CPU (s)	0.1	477	1	9	12
Decision \mathbf{x}	$x_1 = 33.93$	$x_1 = 38.43$	$x_1 = 66.64$	$x_1 = 55.48$	$x_1 = 25.18$
	$x_2 = 29.55$	$x_2 = 27.55$	$x_2 = 62.49$	$x_2 = 52.56$	$x_2 = 33.62$
	$x_3 = 34.30$	$x_3 = 39.92$	$x_3 = 70.87$	$x_3 = 67.60$	$x_3 = 53.14$

* Δ is the data-driven uncertainty budget in the DDANRO approach.

Φ is the data-driven uncertainty budget in the DDNSRO approach.

To compare the optimal solutions obtained from different approaches in an uncertain environment, we perform a simulation with randomly generated 500 uncertainty realizations. These 500 uncertainty realizations are generated in exactly the same way as we generate the original 1,000 labeled uncertainty data points. Specifically, these “testing” uncertainty realizations are from the same 4 data classes as in Figure 3, and the probability distribution for each data class is also the same as the one used to generate the uncertainty data points in Figure 3 such that the two datasets are independently and identically distributed. Although easier to obtain, the deterministic solution leads to infeasibility in 351 out of 500 (70.2%) uncertainty realizations. Due to the two-stage optimization structure, the two-stage stochastic programming approach, the DDANRO and DDNSRO methods could take recourse actions to address the feasibility issue. The simulation results of these three approaches are presented in Figure 5, in which the X-axis is the index of uncertainty realizations, and the Y-axis denotes the deterministic objective value (DOV). The expression for DOV is given in (21).

$$\text{DOV} = 3x_1 + 5x_2 + 6x_3 + 6y_1 + 10y_2 + 12y_3 \quad (21)$$

In Figure 5, the green dots represent the two-stage stochastic programming solutions. We can see that the two-stage stochastic programming approach generates a low DOV under most uncertainty realizations. However, its worst-case DOV is the largest one among all three methods. The brown stars denote the DDANRO solutions. In contrast to the two-stage stochastic programming approach, the DDANRO method performs well under the worst-case uncertainty realization, and its DOV is insensitive to uncertainty. The purple rhombuses represent the

DDNSRO solutions. Under most uncertainty realizations, the purple rhombuses are under the brown stars, which shows that the DDNSRO approach performs better on average than the DDANRO method. The simulation results show that the DDNSRO approach is more suitable to handle labeled multi-class uncertainty data than the DDANRO method. To quantify the performances of different approaches, the simulation results are summarized in Table 2. From Table 2, we can observe that the expected DOV of the two-stage stochastic programming approach is only 6.3% lower than that of the DDNSRO approach. This difference can be considered as the cost for decreasing the worst-case DOV and improving the computational efficiency. The expected DOV of the DDNSRO approach is lower than the DOV of the two-stage ARO method and the one of the DDANRO approach by 26.8% and 18.4%, respectively. The worst-case DOV of DDANRO is the lowest among the three methods. Moreover, all the three robust optimization methods are quite computationally efficient (the resulting problems can be solved within 15 seconds) by leveraging the computational advantage of robust optimization.

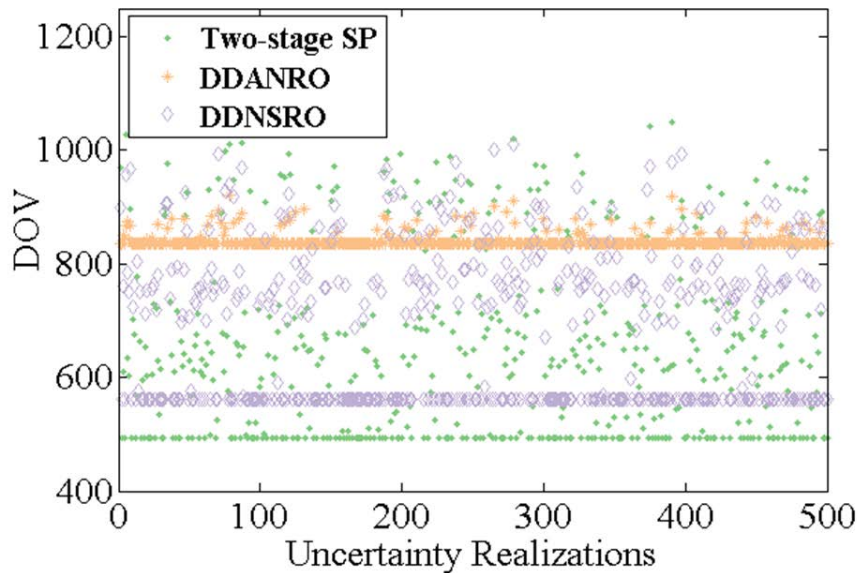


Figure 5. Simulation results for the two-stage stochastic programming approach, the DDANRO and DDNSRO methods with randomly generated 500 uncertainty realizations in the numerical example. SP in the legend represents stochastic programming.

Table 2. Summary of the simulation results in the numerical example.

	Two-stage stochastic programming	Two-stage ARO	DDANRO	DDNSRO
Expected DOV	643.3	937.7	840.8	686.2
Worst-case DOV	1,049.7	957.4	921.6	1,010.6
Standard deviation of DOV	156.7	1.2	14.5	130.6

To demonstrate the computational efficiency of the proposed computational algorithm, we present the upper and lower bounds in each iteration of the tailored C&CG algorithm in Figure 6. The X-axis represents the iteration number, and the Y-axis represents the objective function values. Besides, the relative optimality gaps are listed for each iteration. The relative optimality gap decreases significantly from 32.75% to 3.97% in the first two iterations. As the algorithm iterates, more cuts are added to the master problem. From Figure 6, the proposed computational algorithm takes only 5 iterations to reduce the relative optimality gap to 0.09%, and takes 6 iterations to reach a relative optimality gap of 0.00%. The results clearly demonstrate the efficiency of the proposed computational algorithm.

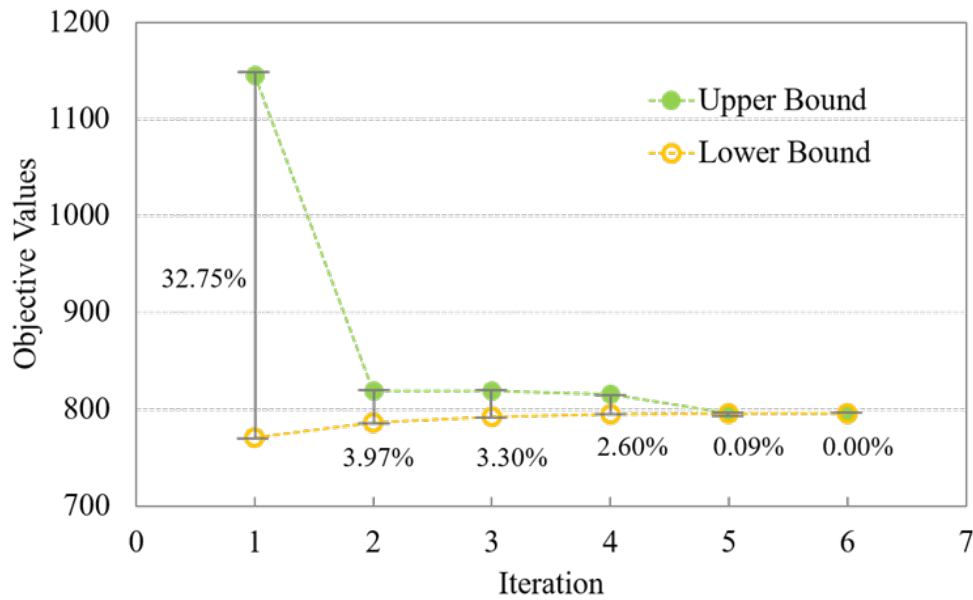


Figure 6. Upper and lower bounds in each iteration of the tailored C&CG algorithm in the numerical example.

Application: Data-Driven Nested Stochastic Robust Planning of Chemical Process Networks under Supply and Demand Uncertainties

In this section, the application of the proposed DDNSRO framework to a multi-period process network planning problem is presented. Large integrated chemical complexes consist of interconnected processes and various chemicals (see Figure 12 for an example).^{52,53} These interconnections allow the chemical production to take advantage of the synergies between different processes.^{54,55} The chemicals in the process network include feedstocks, intermediates and final products. The process network planning determines the purchase levels of feedstocks, sales of final products, capacity expansions, and production profiles of processes at each time period in order to maximize the net present value (NPV) over the strategic planning horizon.⁵⁶ In this application, the supply of feedstocks and demand of products are subject to uncertainty.

Data-driven nested stochastic robust planning of process networks model

The DDNSRO model for process network planning under uncertainty is formulated as follows. The objective is to maximize the NPV, which is given in (22). The constraints can be classified into capacity expansion constraints (23)-(24), budget constraints (25)-(26), production level constraint (27), mass balance constraint (28), supply and demand constraints (29)-(30), non-negativity constraints (31)-(32), and integrity constraint (33). A list of indices/sets, parameters and variables is given in the Notation section, where all the parameters are denoted in lower-case symbols, and all the variables are denoted in upper-case symbols.

The objective function is defined by (22), as shown below.

$$\max_{QE_{it}, Y_{it}} - \sum_{i \in I} \sum_{t \in T} (c1_{it} \cdot QE_{it} + c2_{it} \cdot Y_{it}) + \mathbb{E}_{s \in \Xi} \left[\min_{du_{jt} \in U_s^{\text{dem}}, su_{jt} \in U_s^{\text{sup}}} \max_{P_{sjt}, Q_{sit}, SA_{sjt}, W_{sit}} \left(\sum_{j \in J} \sum_{t \in T} v_{jt} \cdot SA_{sjt} - \sum_{i \in I} \sum_{t \in T} c3_{it} \cdot W_{sit} - \sum_{j \in J} \sum_{t \in T} c4_{jt} \cdot P_{sjt} \right) \right] \quad (22)$$

where QE_{it} is a decision variable for capacity expansion level of process i in time period t , Y_{it} is a binary variable to determine on whether process i is expanded in time period t , SA_{sjt} is the amount of chemical j sold to the market in time period t for data class s , W_{sit} represents the operating level of process i during time period t for data class s , and P_{sjt} is the amount of chemical j purchased in time period t for data class s . Parameters $c1_{it}$, $c2_{it}$, $c3_{it}$ and $c4_{jt}$ are coefficients for variable

investment cost, fixed investment cost, operating cost and purchase cost, respectively. v_{jt} is the sale price of chemical j in time period t .

Constraint (23) enforces the upper and lower bounds of capacity expansions. Specifically, if $Y_{it}=1$, i.e. process i is chosen to be expanded in time period t , the expanded capacity should be within the range $[qe_{it}^L, qe_{it}^U]$.

$$qe_{it}^L \cdot Y_{it} \leq QE_{it} \leq qe_{it}^U \cdot Y_{it}, \quad \forall i, t \quad (23)$$

Constraint (24) specifies the updates of total capacity of each process i .

$$Q_{it} = Q_{i,t-1} + QE_{it}, \quad \forall i, t \quad (24)$$

where Q_{it} is a decision on total capacity of process i in time period t .

Constraints (25) and (26) specify the maximum number of capacity expansions for each process and investment budget for each time period, respectively.

$$\sum_t Y_{it} \leq ce_i, \quad \forall i \quad (25)$$

$$\sum_t (c1_{it} \cdot QE_{it} + c2_{it} \cdot Y_{it}) \leq cb_t, \quad \forall t \quad (26)$$

where ce_i is the maximum expansion times for process i , and cb_t is the investment budget for time period t .

Constraint (27) enforces that the production level of a process cannot exceed its total capacity.

$$W_{sit} \leq Q_{it}, \quad \forall s, i, t \quad (27)$$

Constraint (28) specifies the mass balance for chemicals. To be more specific, the purchase amount plus the production amount is equal to the total amount sold to the market and consumed by processes.

$$P_{sjt} - \sum_i \kappa_{ij} \cdot W_{sit} - SA_{sjt} = 0, \quad \forall s, j, t \quad (28)$$

where κ_{ij} is the mass balance coefficient for chemical j in process i .

Constraint (29) enforces that the purchase amount of a feedstock should not be higher than its available amount provided by the supplier. Constraint (30) specifies that the sale amount of a product cannot exceed its market demand.

$$P_{sjt} \leq su_{jt}, \quad \forall s, j, t \quad (29)$$

$$SA_{sjt} \leq du_{jt}, \quad \forall s, j, t \quad (30)$$

where su_{jt} is the market availability and du_{jt} is the demand of chemical j in time period t .

Constraints (31)-(32) indicate the non-negativity of continuous decisions.

$$QE_{it} \geq 0, Q_{it} \geq 0 \quad \forall i, t \quad (31)$$

$$P_{sjt}, SA_{sjt}, W_{sit} \geq 0, \quad \forall s, j, t \quad (32)$$

Constraint (33) ensures that Y_{it} is a binary variable.

$$Y_{it} \in \{0, 1\}, \quad \forall i, t \quad (33)$$

Uncertainty information for demand and supply uncertainties is shown in (34)-(35).

$$U_s^{\text{dem}} = \bigcup_{k: \gamma_{s,k}^{\text{dem}} \geq \gamma^*} \left\{ \mathbf{d}\mathbf{u} \mid \mathbf{d}\mathbf{u} = \boldsymbol{\mu}_{s,k}^{\text{dem}} + \boldsymbol{\kappa}_{s,k}^{\text{dem}} \cdot \sqrt{\boldsymbol{\Psi}_{s,k}^{\text{dem}}} \cdot \boldsymbol{\Lambda}_{s,k}^{\text{dem}} \cdot \mathbf{z}, \|\mathbf{z}\|_{\infty} \leq 1, \|\mathbf{z}\|_1 \leq \Phi_{s,k}^{\text{dem}} \right\} \quad (34)$$

where $\boldsymbol{\mu}_{s,k}^{\text{dem}}$, $\boldsymbol{\kappa}_{s,k}^{\text{dem}}$, $\boldsymbol{\Psi}_{s,k}^{\text{dem}}$ are the inference results learned from uncertain product demand data using the Variational inference algorithm.

$$U_s^{\text{sup}} = \bigcup_{k: \gamma_{s,k}^{\text{sup}} \geq \gamma^*} \left\{ \mathbf{s}\mathbf{u} \mid \mathbf{s}\mathbf{u} = \boldsymbol{\mu}_{s,k}^{\text{sup}} + s_{s,k}^{\text{sup}} \cdot \sqrt{\boldsymbol{\Psi}_{s,k}^{\text{sup}}} \cdot \boldsymbol{\Lambda}_{s,k}^{\text{sup}} \cdot \mathbf{z}, \|\mathbf{z}\|_{\infty} \leq 1, \|\mathbf{z}\|_1 \leq \Phi_{s,k}^{\text{sup}} \right\} \quad (35)$$

where $\boldsymbol{\mu}_{s,k}^{\text{sup}}$, $\boldsymbol{\kappa}_{s,k}^{\text{sup}}$, $\boldsymbol{\Psi}_{s,k}^{\text{sup}}$ are the inference results learned from uncertain supply data employing the Variational inference algorithm. The probabilities of different data classes are extracted using sample proportions.

The resulting problem on strategic planning of process network under uncertainty is a multi-level MILP. Due to the multi-level optimization structure, it cannot be solved directly by any off-the-shelf optimization solvers. The proposed computational algorithm is used to solve this large-scale optimization problem. In the next two subsections, two case studies are presented to demonstrate the applicability of the DDNSRO approach.

Case study 1

A small-scale case study is presented in this subsection. The process network, which is shown in Figure 7, consists of 5 chemicals, 3 processes, 3 suppliers and 2 markets.⁵³ In Figure 7, chemicals A-C represent raw materials, which can be either purchased from certain suppliers or produced by processes. For example, Chemical C can be either manufactured by Process 3 or purchased from a supplier. Chemicals D and E are final products, which are sold to the markets. In this case study, we consider 10 time periods over the 20-year planning horizon, and the duration of each time period is 2 years. It is assumed that processes do not have initial capacities, and they can be installed at the beginning of time period 1.

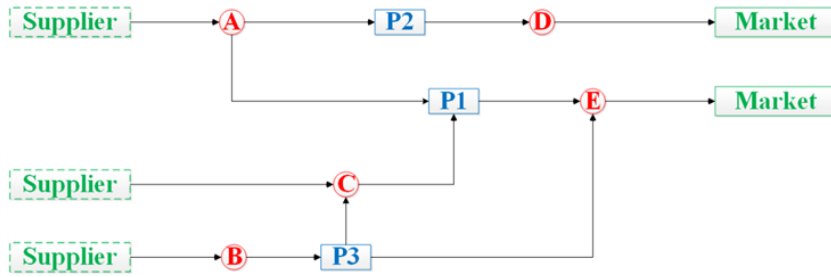


Figure 7. The chemical process network of case study 1.

Due to market fluctuations, the supplies of feedstocks A-C, and demands of products D-E are subject to uncertainty. A total of 160 demand uncertainty data are used in this case study, and each data point corresponds to a combination of all product demand realizations. For the supply uncertainty, 200 uncertainty data points are used. Each data point represents a combination of supply uncertainty realizations for all feedstocks. There are 2 labels within demand uncertainty data, which indicates 2 data classes. There are also 2 data classes within the supply uncertainty data.

By employing the proposed data-driven uncertainty modeling framework, we obtain the uncertainty modeling results for demand and supply uncertainties in Figure 8 and Figure 9, respectively. In these two figures, the red dots and red stars represent uncertainty data from different data classes, and the polytopes represent data-driven uncertainty sets with uncertainty budgets $\Phi^{\text{dem}}=1$ and $\Phi^{\text{sup}}=1$. Due to the settings of uncertainty budgets, some data points are not included in the uncertainty sets. The occurrence probabilities of different data classes are inferred from the label information, and the corresponding numerical values are listed in the two figures. From Figure 8, we can see that that the probabilities of demand data classes 1 - 2 are 0.5 and 0.5, respectively. There is only one component in the Dirichlet process mixture model for both data classes 1 and 2. The proposed uncertainty model accurately capture the correlations among the two uncertain parameters for demands. Figure 9 shows that the occurrence probabilities for the two supply data classes are the same. There is one component in each of these data classes. The DDNSRO problem for the planning of process network can be solved with the data-driven uncertainty information in Figure 8 and Figure 9.

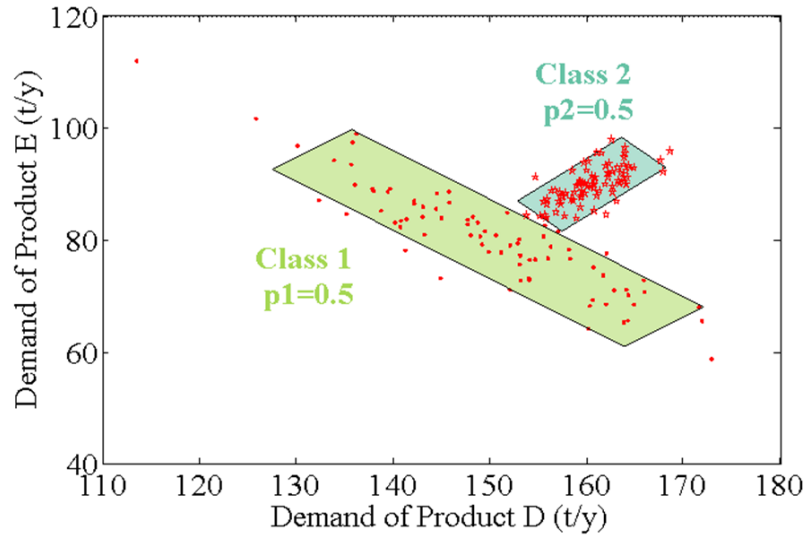


Figure 8. The data-driven demand uncertainty modeling results ($\Phi^{\text{dem}}=1$) for the two data classes in case study 1.

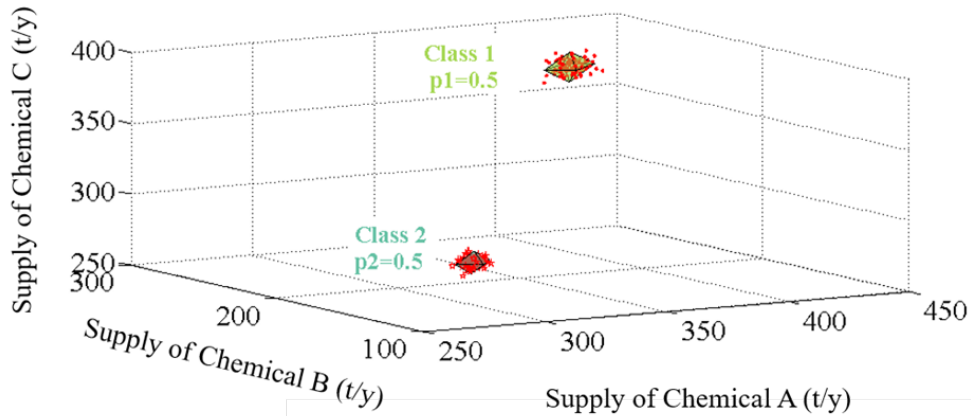


Figure 9. The data-driven supply uncertainty modeling results ($\Phi^{\text{sup}}=1$) for the two data classes in case study 1.

To demonstrate the advantages of the proposed approach, we solve the optimization problem of process network planning using the deterministic optimization method, the two-stage ARO method with a box set, the two-stage stochastic programming method, the DDANRO approach, and the DDNSRO approach. All optimization methods are modeled in GAMS 24.7.3,⁵⁷ and are implemented on a computer with an Intel (R) Core (TM) i7-6700 CPU @ 3.40 GHz and 32 GB

RAM. The relative optimality gaps for both the tailored C&CG algorithm and the multi-cut Benders decomposition algorithm are set to be 0.1%.

The computational results and model statistics are summarized in Table 3. For the two-stage stochastic programming problem, each scenario corresponds to the combination of a demand uncertainty data point and a supply uncertainty data point. There are 32,000 (160×200) scenarios in the two-stage stochastic programming problem, and each scenario is assigned with the same probability. Two-stage stochastic programming approach aims to get a solution that performs well on average, so its objective value is only 3.7% higher than that of the DDNSRO approach. However, it takes 28 iterations and 106,140 seconds to solve the resulting two-stage stochastic programming problem with the multi-cut Benders decomposition.⁵¹ By contrast, the DDNSRO problem can be solved within only 3 seconds, which demonstrates its computational advantage. As more uncertainty data are considered and the scale of the problem becomes larger (e.g. case study 2), the computational advantage of DDNSRO over the two-stage stochastic programming approach is more prominent.

Table 3. Comparisons of model and solution statistics between different methods in in case study 1.

	Deterministic Planning	Two-stage stochastic programming		Two-stage ARO		DDANRO ($\Delta^{\text{dem}}=1, \Delta^{\text{sup}}=1$)*		DDNSRO ($\Phi^{\text{dem}}=1, \Phi^{\text{sup}}=1$)#	
		Master problem	Sub-problem	Master problem	Sub-problem	Master problem	Sub-problem	Master problem	Sub-problem
Bin. Var.	30	30	0	30	5	30	20	30	20
Cont. Var.	196	32,061	131	322	386	582	1,181	582	1,181
Constraints	276	864,091	181	453	433	815	3,143	813	3,143
Max. NPV (\$K)	1,809.5		1,802.6		1,372.5		1,671.7		1,739.1
Total CPU (s)	0.2		106,140		1		7		3
Iterations	N/A		28		2		4		2

* Δ^{dem} and Δ^{sup} are data-driven uncertainty budgets in the DDANRO approach for demand and supply, respective.

Φ^{dem} and Φ^{sup} are data-driven uncertainty budgets in the DDNSRO approach for demand and supply, respective.

The optimal capacity expansion decisions determined by the two-stage stochastic programming approach, the DDANRO and DDNSRO approaches are shown in Figure 10 (a), (b) and (c), respectively. As can be observed from Figure 10, Process 1 is expanded at time period 5, and Process 2 starts the expansion at time period 2 for all the three methods. Moreover, Process 2 is further expanded at the sixth time period in the solution determined by the DDNSRO approach. By contrast, Process 2 is not chosen to be expanded from time period 2 in the DDANRO solution. The optimal process capacities for the last time period determined by the two-stage stochastic programming approach, the DDANRO and DDNSRO methods are listed in Table 4.

Table 4. The optimal capacity of processes at time period 10 in case study 1.

Process Capacity (t/y)	Two-stage stochastic programming	DDANRO	DDNSRO
Process 1	100	114	114
Process 2	227	207	225
Process 3	51	39	39

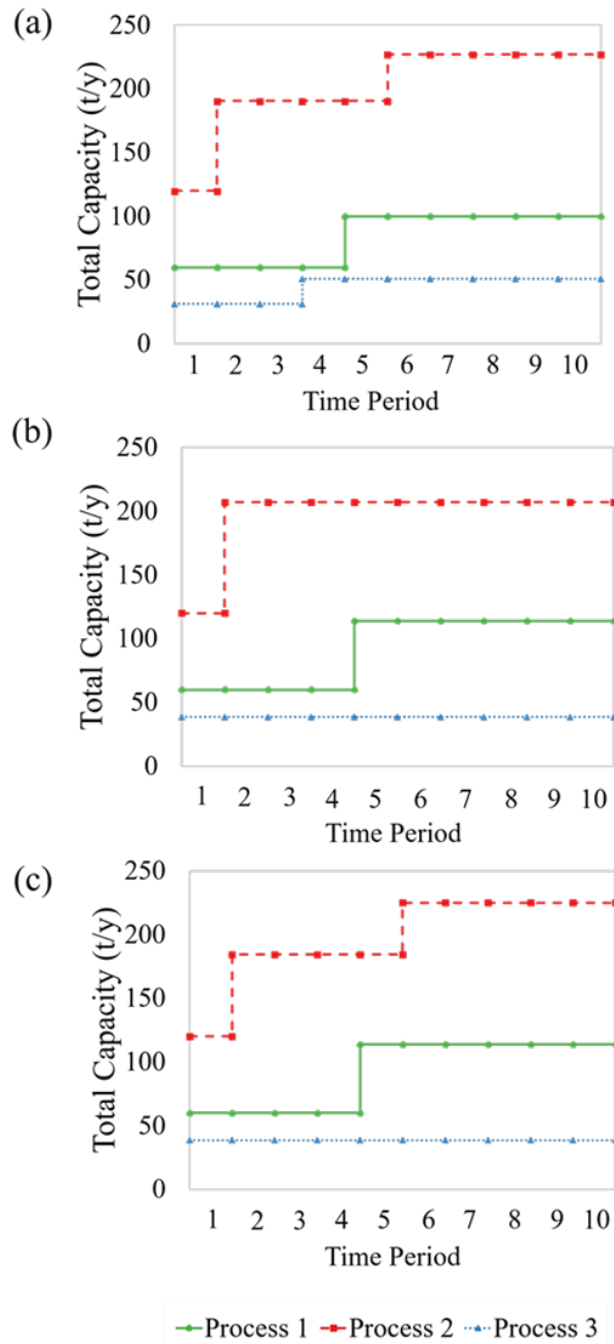


Figure 10. Optimal capacity expansion decisions over the entire planning horizon determined by (a) the two-stage stochastic programming approach (b) the DDANRO approach, and (c) the DDNSRO approach in case study 1.

The details on revenues and cost breakdown, including fixed investment cost, variable investment cost, operating cost, and purchase cost, are shown in Figure 11. As can be seen from

the bar chart, the deterministic method returns the highest revenue by considering only one uncertainty realization, which is the mean value of the multi-class uncertainty data. From the pie charts in Figure 11, we can observe that more than 60% of the total cost comes from purchasing feedstocks for all methods. Moreover, the percentage of the operating cost for the DDANRO method is 1% lower than those determined by the other two approaches.

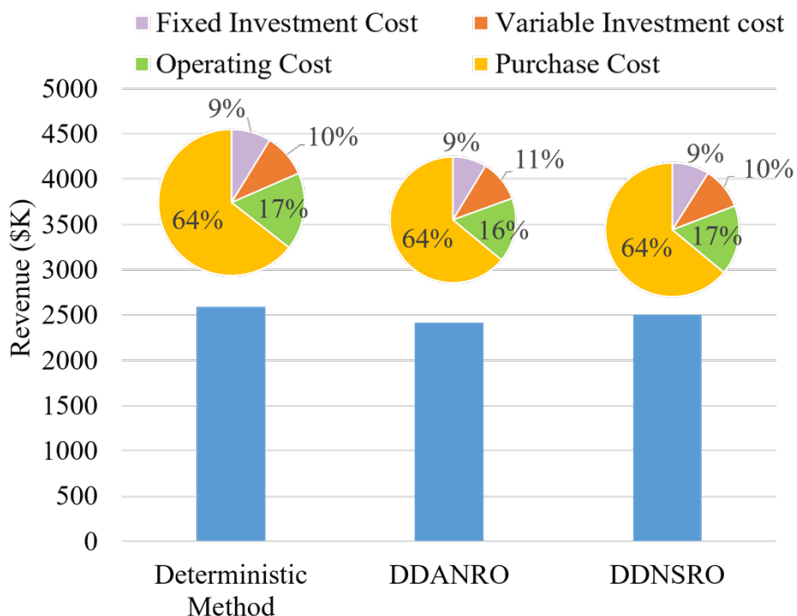


Figure 11. Revenues and cost break down determined by different methods in case study 1.

Case study 2

A large-scale case study is presented in this subsection to demonstrate the advantages of the DDNSRO approach. The process network in this case study consists of 28 chemicals, 38 processes, 10 suppliers and 16 markets,⁵³ as shown in Figure 12. In Figure 12, Chemicals A-J represent raw materials, which can be purchased from suppliers or manufactured by certain processes. Chemicals K-Z are final products, which are sold to the markets. The intermediates are denoted as AA and AB. This complex process network has such flexibility that many manufacturing options are available. For example, Chemical L can be manufactured by Process 2, Process 15 and Process 17. In this case study, we consider 10 time periods over the planning horizon, and the duration of each time period is 2 years. It is assumed that processes 12, 13, 16 and 38 have initial capacities of 40, 25, 300 and 200 kt/y, respectively, at the beginning of time period 1. These processes cannot be

expanded until time period 2. The other processes can be installed at the beginning of time period 1.

As in the previous case study, supplies of all feedstocks and demands of all final products are subject to uncertainty. For the supply uncertainty, a total of 4,000 uncertainty data are used for uncertainty modeling. Each data point has 10 dimensions for a combination of all feedstocks. For the demand uncertainty, 4,000 uncertainty data points are used, and each data point is for a combination of all the 16 products. There are 3 labels within demand uncertainty data, which indicates 3 data classes. There are also 3 data classes within the supply uncertainty data.

The occurrence probabilities of different data classes are inferred from the label information. The data-driven uncertainty modeling results show that the probabilities of supply data classes 1 - 3 are 0.25, 0.50, and 0.25, respectively. There is one component in the Dirichlet process mixture models for all supply data classes. The probabilities of demand data classes 1 - 3 are calculated to be 0.25, 0.50, and 0.25, respectively. The number of components in the Dirichlet process mixture models is one for all demand data classes. The extracted uncertainty information is incorporated into the DDNSRO based planning problem.

To demonstrate the advantages of the proposed DDNSRO framework, we solve the process network planning problem using deterministic method, the two-stage ARO approach, the two-stage stochastic programming approach, the DDANRO method and the DDNSRO approach. As in the previous case study, the relative optimality gaps for the tailored C&CG algorithm and multi-cut Benders decomposition algorithm are set to be 0.1%. In the two-stage stochastic programming problem, there are $1.6E+7$ scenarios (4000×4000), and the probability of each scenario is given as $6.25E-8$. In the deterministic equivalent of the two-stage stochastic programming problem, there are 380 integer variables, 15,040,000,760 continuous variables, and 19,520,001,140 constraints. The size of this two-stage stochastic programming problem is too large to be solved within the computational time limit of 48 hours using the multi-cut Benders decomposition algorithm. Consequently, its results are not presented. The computational results and model statistics are presented in Table 5.

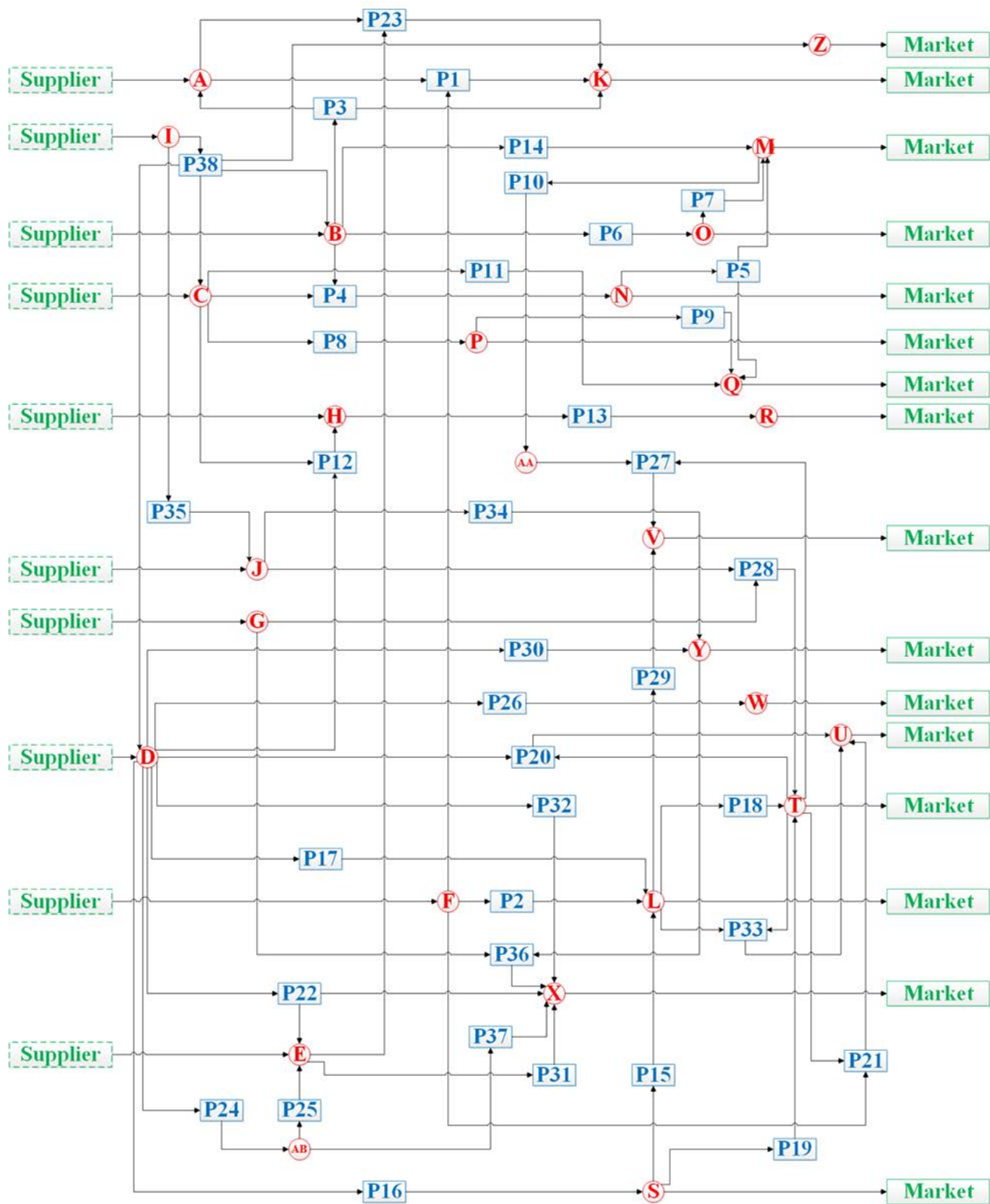


Figure 12. The chemical process network of case study 2.

Table 5. Comparisons of model and solution statistics between different methods in case study 2.

	Deterministic Planning	Two-stage ARO		DDANRO ($\Delta^{\text{dem}}=5, \Delta^{\text{sup}}=3$) [#]		DDNSRO ($\Phi^{\text{dem}}=5, \Phi^{\text{sup}}=3$) [#]	
		Master problem	Sub-problem	Master problem	Sub-problem	Master problem	Sub-problem
Bin. Var.	380	380	30	380	112	380	112
Cont. Var.	1,706	6,402	2,367	13,922	32,581	120,42	32,581
Constraints	2,366	8,467	2,623	18,235	95,097	15,785	95,079
Max. NPV (\$M)	2,203.6		740.5		786.8		1,844.2
Total CPU (s)	0.4		12		3,065		557
Iterations	N/A		6		14		4

* Δ^{dem} and Δ^{sup} are data-driven uncertainty budgets in the DDANRO approach for demand and supply, respective.

Φ^{dem} and Φ^{sup} are data-driven uncertainty budgets in the DDNSRO approach for demand and supply, respective.

From Table 5, we can see that the deterministic planning method consumes less computational time, and generates the highest NPV. However, its solution suffers from infeasibility issue if the supply of raw materials and demand of final products are uncertain. By leveraging the corresponding strengths of two-stage stochastic programming approach and the two-stage ARO method, the DDNSRO approach generates \$1,057.4M higher NPV than the solution from the DDANRO method, while maintaining the computational tractability. The DDNSRO problem can be solved within only 10 minutes using the proposed computational algorithm. The optimal design and planning decisions for time period 10 determined by the deterministic optimization method, DDANRO, and DDNSRO approaches are shown in Figure 13, Figure 14 and Figure 15, respectively. In these three figures, the optimal total capacities are displayed under operating processes.

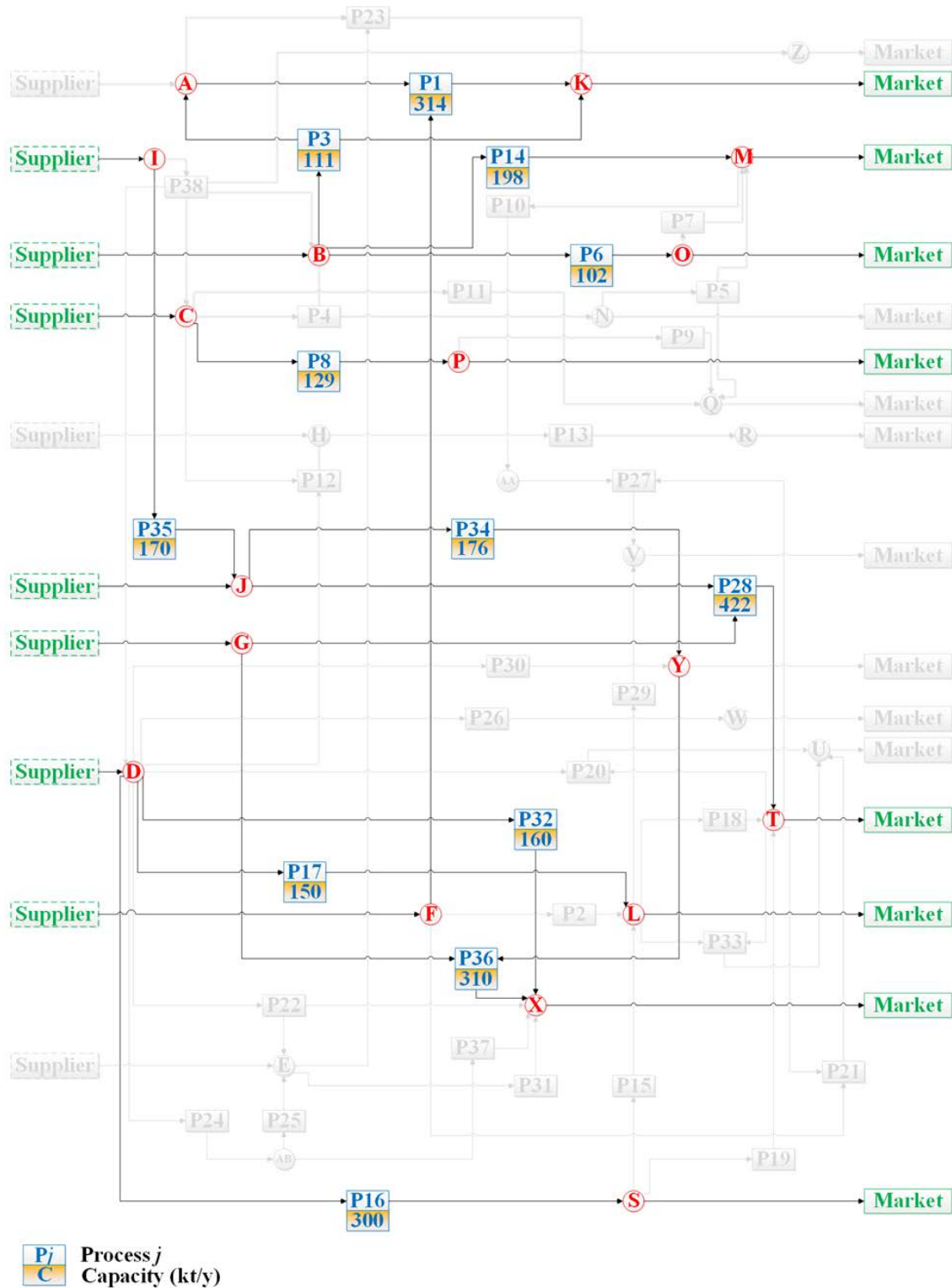


Figure 13. The optimal design and planning decisions for time period 10 determined by the deterministic optimization method in case study 2.

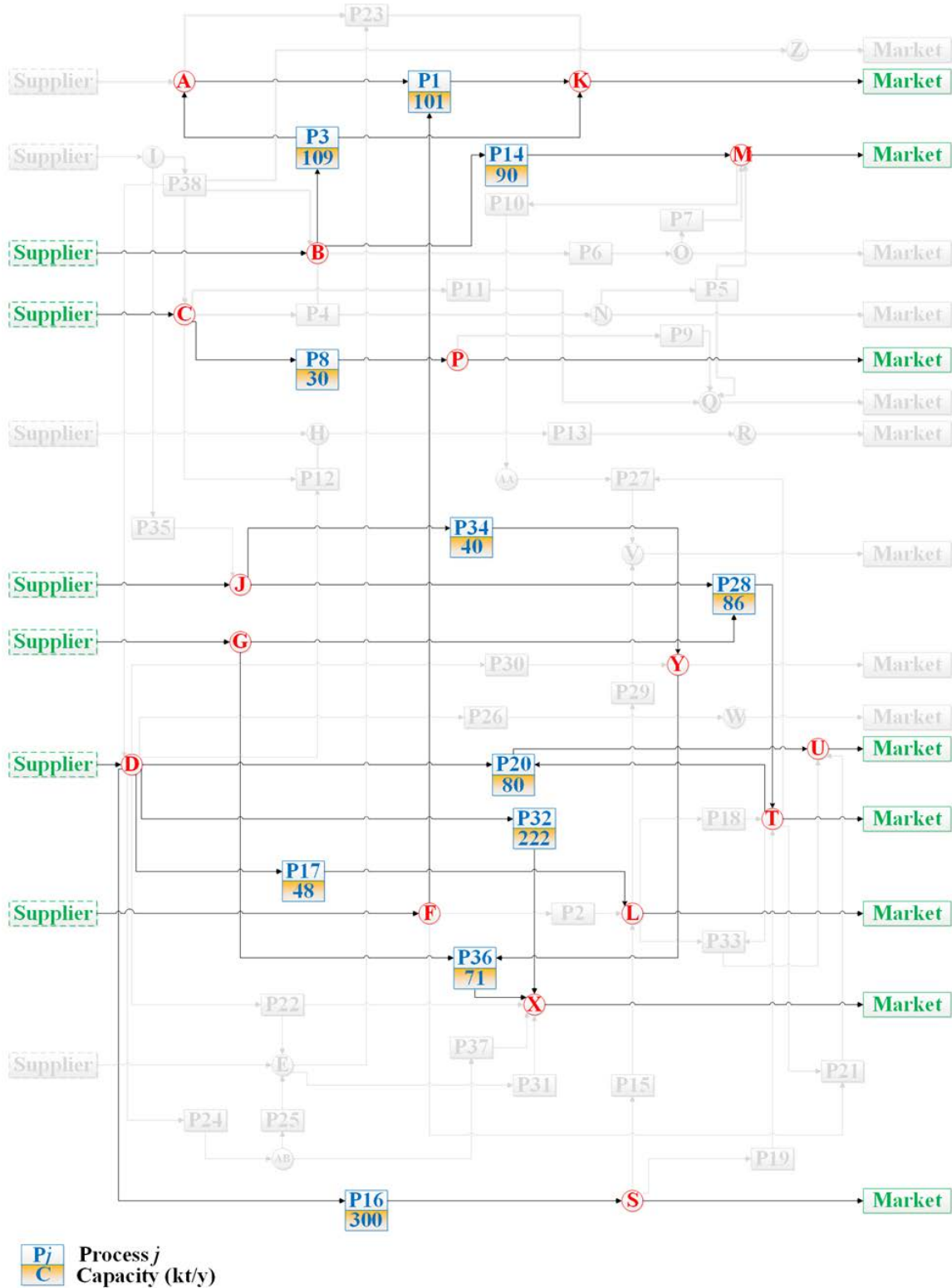


Figure 14. The optimal design and planning decisions for time period 10 determined by the DDANRO approach in case study 2.

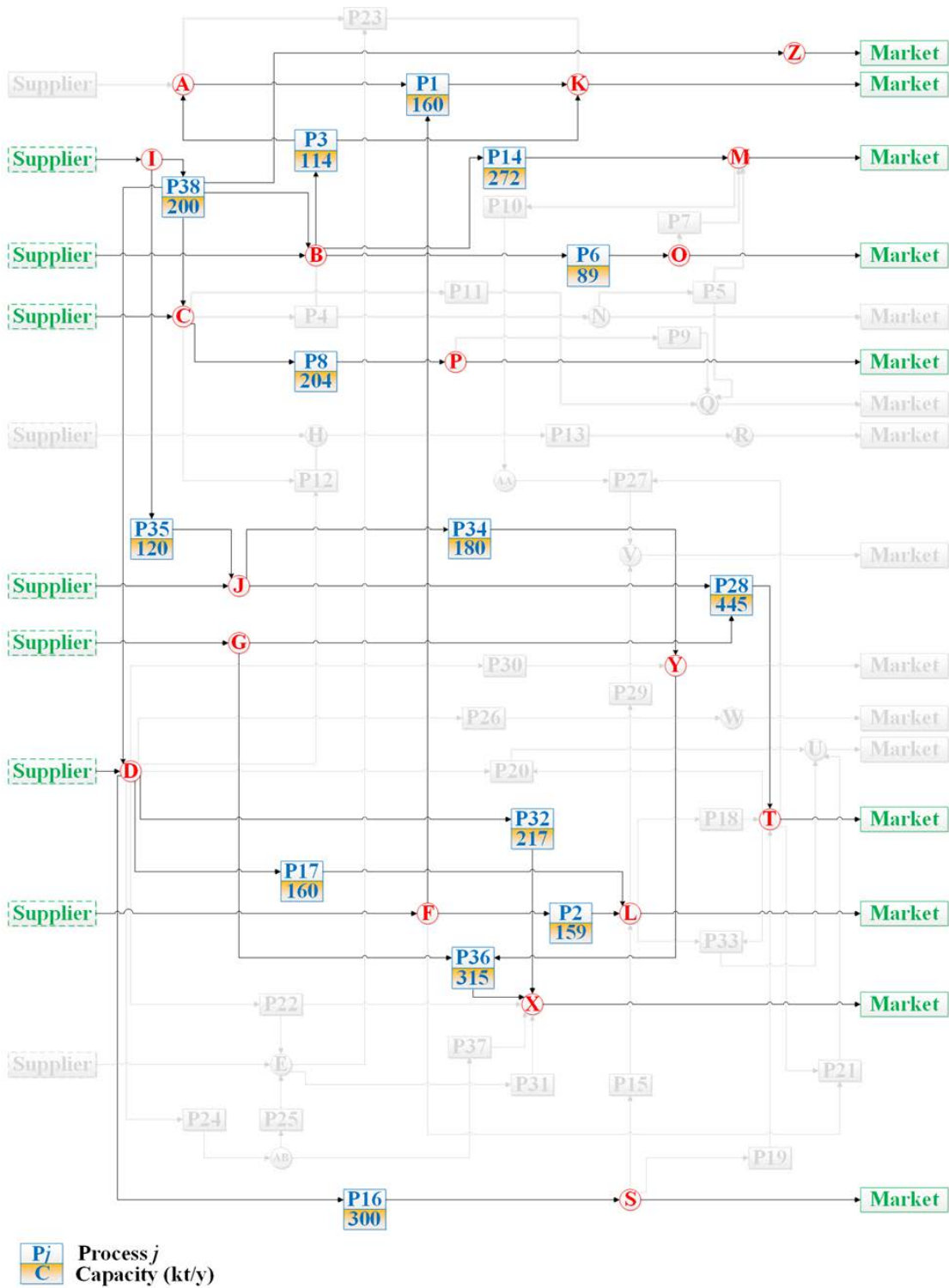


Figure 15. The optimal design and planning decisions for time period 10 determined by the proposed DDNSRO approach in case study 2.

The optimal capacity expansion decisions determined by the DDANRO method and the DDNSRO approach are shown in Figure 16 and Figure 17, respectively. From Figure 16, we can see that a total of 15 processes are selected in the optimal process network determined by the DDANRO method. As shown in Figure 17, a total of 18 processes are chosen in the optimal process network determined by the DDNSRO approach. Specifically, Processes 2, 6 and 11 are not selected in the optimal process network determined by the DDANRO method. Besides, the optimal expansion frequencies and total capacities of Process 28 determined by the two methods are different.

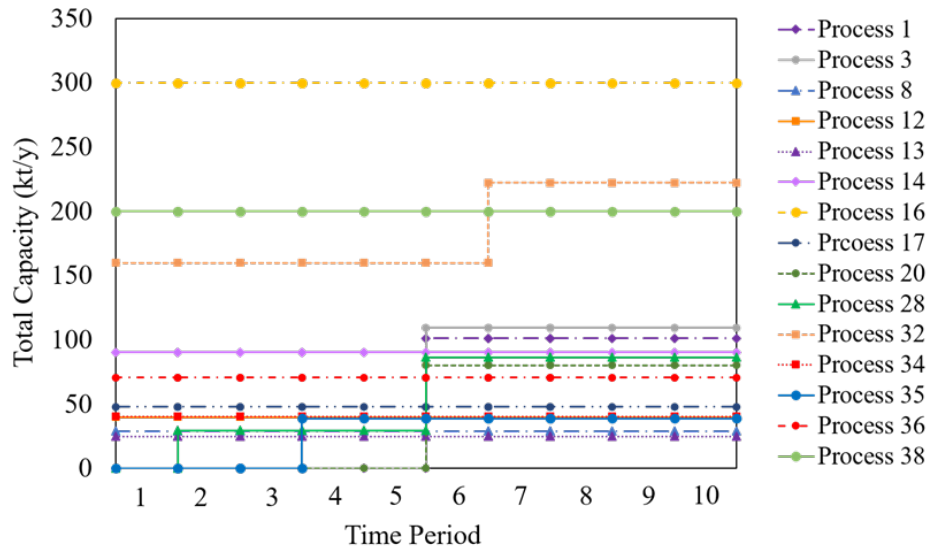


Figure 16. Optimal capacity expansion decisions over the entire planning horizon determined by the DDANRO approach in case study 2.

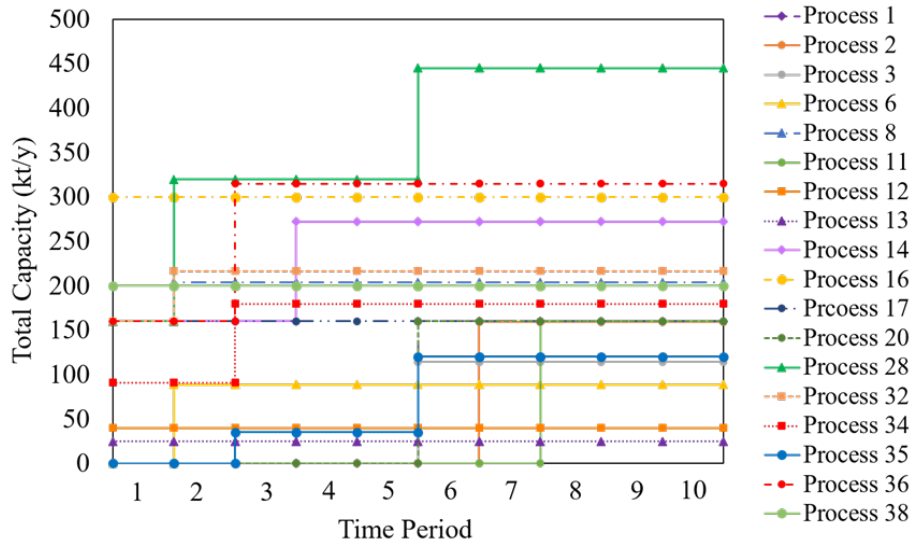


Figure 17. Optimal capacity expansion decisions over the entire planning horizon determined by the proposed DDNSRO approach in case study 2.

The details on revenues and cost breakdown are shown in Figure 18. From the pie charts in Figure 18, we can see that more than half of the total cost is from purchasing raw materials for the three approaches. The investment costs for the deterministic method, the DDANRO and DDNSRO methods are \$338.4M, \$142.3M and \$323.1M, respectively. The lower capital costs of the DDANRO method can be explained by the fewer selected processes and the lower capacities compared with the other two methods.

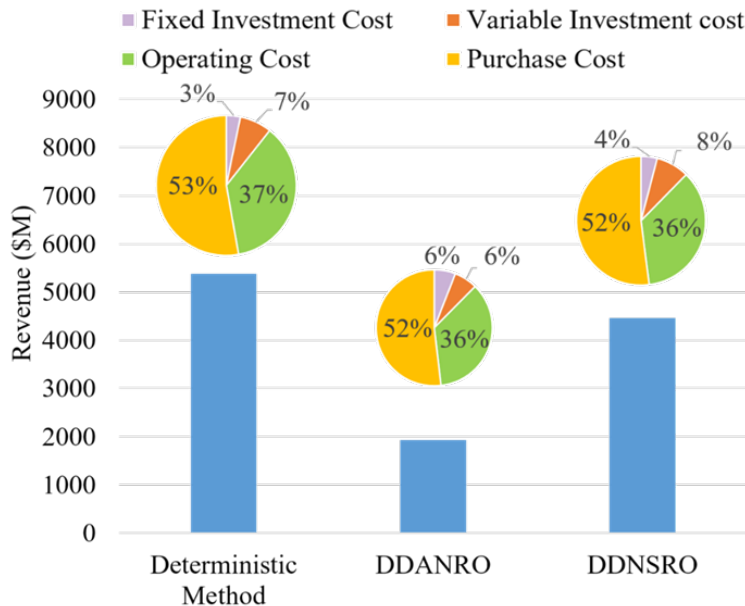


Figure 18. Revenues and cost break down determined by different methods in case study 2.

To demonstrate the superior performance of the DDNSRO approach over the DDANRO method in an uncertain environment, we perform a simulation with randomly generated 1,000 uncertainty realizations. These 1,000 uncertainty realizations are generated in exactly the same way as we generate the original uncertainty data points for uncertainty modeling. Specifically, the “testing” uncertainty realizations are from the same 3 data classes as the uncertainty data used for data-driven uncertainty modeling, and the probability distribution for each data class is also the same to ensure that the uncertainty data for modeling and for simulation are independently and identically distributed. The simulation results are shown in Figure 19, in which the X-axis denotes the index of uncertainty realizations, and the Y-axis denotes the NPV. The statistics of the simulation results are provided in Table 6. In the figure, the green stars represent the DDANRO solutions, while the brown rhombuses represent the DDNSRO solutions. The DDNSRO approach generates a higher NPV than that of the DDANRO method under 789 out of 1,000 uncertainty realizations. We also plot the average NPV over all the 1,000 uncertainty realizations for the DDANRO and DDNSRO approaches, as given by the red dashed horizontal line and blue horizontal line, respectively. The DDNSRO approach generates \$838.1M higher expected NPV than that of the DDANRO method, while the worst-case NPV is merely \$86.1M lower compared with that of the DDANRO method. The above simulation results clearly demonstrate that the DDNSRO approach compares favorably with the DDANRO method in handling labeled multi-class uncertainty data.

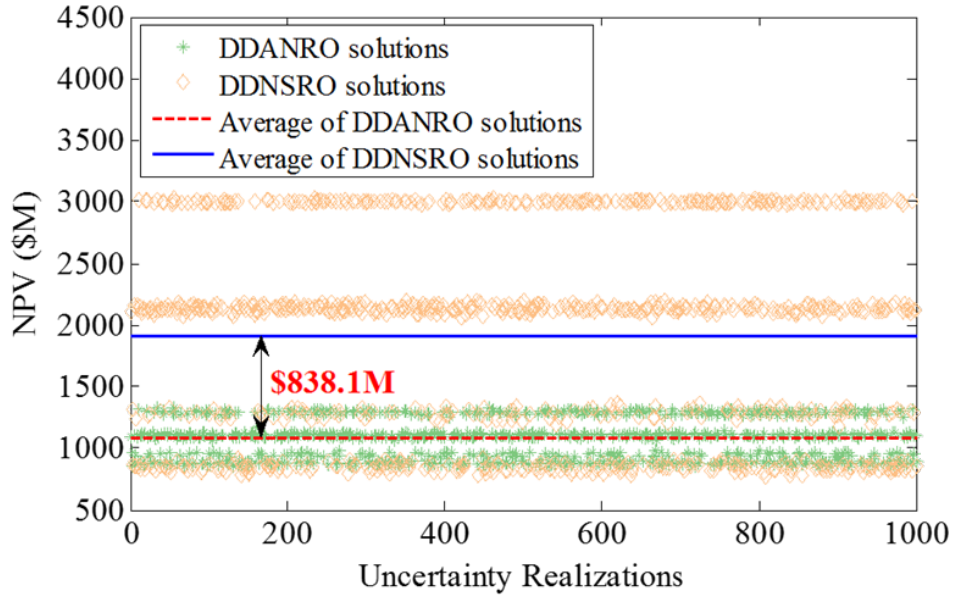


Figure 19. Simulation results for the DDANRO and DDNSRO approaches with randomly generated 1,000 “testing” uncertainty realizations that are independently and identically distributed as the uncertainty data used for data-driven uncertainty modeling in case study 2.

Table 6. Summary of the simulation results in case study 2.

	Two-stage ARO	DDANRO	DDNSRO
Expected NPV (\$M)	939.6	1072.1	1910.2
Worst-case NPV (\$M)	753.6	853.4	767.3
Standard deviation of NPV (\$M)	134.6	154.0	800.7

To demonstrate the computational performance of the proposed computational algorithm, we display the upper and lower bounds in each iteration of the proposed algorithm in Figure 20. The X-axis represents the iteration number, and the Y-axis represents the objective function values. In Figure 20, the green dots stand for the upper bounds, and the yellow circles represent the lower bounds. The proposed solution algorithm requires only 4 iterations to converge. During the first two iterations, the relative optimality gap decreases significantly from 88.01% to 0.67%. The proposed solution algorithm takes only 3 iterations to reduce the relative optimality gap to 0.60%, and requires 4 iterations to reach a relative optimality gap below the predefined relative optimality gap of 0.1%. The results demonstrate the efficiency of the proposed computational algorithm.

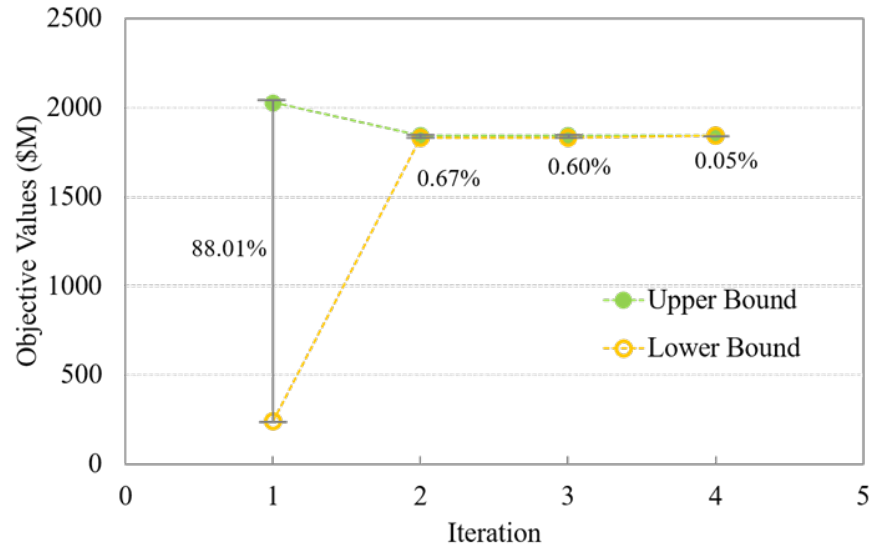


Figure 20. Upper and lower bounds in each iteration of the tailored C&CG algorithm in case study 2.

To investigate how the optimal solution varies with the uncertainty budget parameters, a heat map of solutions under different supply and demand budgets is shown in Figure 21. It is clear to see that increasing either the supply or demand uncertainty budget leads to a lower NPV. The solutions toward the upper right corner have a smaller NPV and are more conservative. The solutions toward the lower left corner have a larger NPV and are less conservative. Viewing by columns, we can see that increasing the uncertainty budget for supply does not change the objective value significantly. Viewing by rows, increasing the uncertainty budget for demands reduces the NPV considerably. Comparing the magnitudes of these changes in objective values, we conclude that the impact of the demand uncertainty budget on NPV is more significant than that of the supply uncertainty budget.

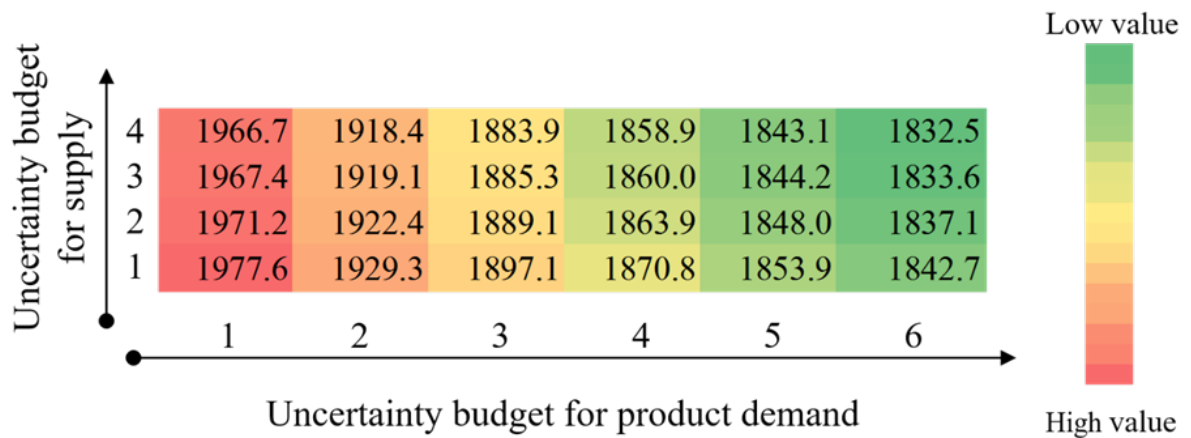


Figure 21. Heat map of solutions under different budgets for the DDNSRO approach in case study 2.

Conclusions

In this paper, a novel DDNSRO framework was proposed for labeled multi-class uncertainty data. Instead of handling all uncertainty data homogeneously, the proposed framework explicitly accounted for the label information in the proposed multi-level optimization model. The probability distribution for data classes was learned from uncertainty data through maximum likelihood estimation. A group of Dirichlet process mixture models was used to construct uncertainty sets for each data class. The proposed data-driven nonparametric uncertainty model was capable to automatically adapt its complexity based on data structure, thus accurately extracting the useful information from uncertainty data. Two-stage stochastic programming approach was nested in the outer optimization problem, aiming to balance different data classes based on their occurrence probabilities. To handle high-dimensional uncertainties in each data class, robust optimization was nested in the inner optimization problem for the robustness of the solution and computational tractability. The proposed DDNSRO framework leveraged the advantages of two-stage stochastic programming approach and robust optimization, and at the same time exploited the value of big data. Since the resulting DDNSRO problem has multi-level structure, we further proposed a tailored C&CG algorithm to address the computational challenge. We presented a numerical example and two case studies on strategic planning of process networks under supply and demand uncertainties. The results show that the DDNSRO approach was

advantageous over the DDANRO method in handling labeled multi-class uncertainty data, and was more computationally efficient than two-stage stochastic programming approach.

Acknowledgments

The authors acknowledge financial support from the National Science Foundation (NSF) CAREER Award (CBET-1643244).

Appendix A: The Variational Inference Algorithm

In this appendix, the details of variational inference algorithm for the Dirichlet process mixture model are provided. Suppose $\Theta = (\mathbf{l}, \boldsymbol{\beta}, \alpha, \boldsymbol{\eta}, \mathbf{H})$ is set of all latent variables and parameters of the Dirichlet process mixture model, and $\mathbf{U} = (\mathbf{u}_1, \dots, \mathbf{u}_N)$ are the observations of uncertain parameters. The Dirichlet process mixture model, specifies the distribution $p(\mathbf{U}, \Theta)$. From a Bayesian perspective, the goal of inference is to find the posterior distribution of Θ given the observation data \mathbf{U} , that is $p(\Theta|\mathbf{U})$. In the variational inference, the log marginal probability is decomposed into two parts.

$$\log p(\mathbf{U}) = \text{ELBO}(q) + \text{KL}(q\|p) \quad (\text{A1})$$

where the first part is called the evidence lower bound (ELBO), and the second part is Kullback-Leibler divergence or KL divergence; q is the variational distribution to approximate the posterior distribution $p(\Theta|\mathbf{U})$. They are defined as follows.^{46,58}

$$\text{ELBO}(q) = \int q(\Theta) \log \left\{ \frac{p(\mathbf{U}, \Theta)}{q(\Theta)} \right\} d\Theta \quad (\text{A2})$$

$$\text{KL}(q\|p) = - \int q(\Theta) \log \left\{ \frac{p(\Theta|\mathbf{U})}{q(\Theta)} \right\} d\Theta \quad (\text{A3})$$

Given the $\text{KL}(q\|p)$ is a distance between the distributions q and p , the goal of the variational algorithm is to minimize $\text{KL}(q\|p)$ to achieve the best approximation. Since $\log p(\mathbf{U})$ is a constant with respect to q , minimizing the KL divergence levels to maximizing the ELBO. To obtain a tractable inference, the variational inference utilize a factorized variational distribution $q(\mathbf{l}, \boldsymbol{\beta}, \alpha, \boldsymbol{\eta}, \mathbf{H})$.

$$q(\alpha) = \text{Gamma}(\chi_1^*, \chi_2^*) \quad (\text{A4})$$

where Gamma represents the Gamma distribution, and the hyper-parameters are updated by

$$\chi_1^* = \chi_1 + M - 1 \quad (\text{A5})$$

$$\chi_2^* = \chi_2 - \sum_{i=1}^{M-1} \langle \ln(1 - \beta_i) \rangle \quad (\text{A6})$$

The notation $\langle \cdot \rangle$ represents the expectation of corresponding random variable. All closed forms of $\langle \cdot \rangle$ are listed at the end of Appendix A.

The posterior of β_k is as follows.

$$q(\beta_k) = \text{Beta}(\tau_k, \nu_k) \quad (\text{A7})$$

where Beta represents the Beta distribution, and the hyper-parameters are updated by

$$\tau_k^* = 1 + \sum_{n=1}^N q(l_n = k) \quad (\text{A8})$$

$$\nu_k^* = \langle \alpha \rangle + \sum_{n=1}^N \sum_{i=k+1}^M q(l_n = i) \quad (\text{A9})$$

The posterior of $q(\boldsymbol{\eta}_k, \mathbf{H}_k)$ is the Normal-Wishart distribution, and the related parameters are calculated in (A11)-(A15).

$$q(\boldsymbol{\eta}_k, \mathbf{H}_k) = \mathcal{N}\left(\boldsymbol{\eta}_k \mid \boldsymbol{\mu}_k^*, (\lambda_k^* \boldsymbol{\Psi}_k^{*-1})^{-1}\right) \mathcal{W}\left(\mathbf{H}_k \mid \boldsymbol{\Psi}_k^{*-1}, \omega_k^*\right) \quad (\text{A10})$$

$$N_k = \sum_{n=1}^N q(l_n = k) \quad (\text{A11})$$

$$\lambda_k^* = \lambda_k + N_k \quad (\text{A12})$$

$$\omega_k^* = \omega_k + N_k \quad (\text{A13})$$

$$\boldsymbol{\mu}_k^* = \frac{1}{\lambda_k^*} \left(\lambda_k \boldsymbol{\mu}_k + \sum_{n=1}^N q(l_n = k) \mathbf{u}_n \right) \quad (\text{A14})$$

$$\boldsymbol{\Psi}_k^* = \boldsymbol{\Psi}_k + \sum_{n=1}^N q(l_n = k) \left(\mathbf{u}_n - \frac{1}{N_k} \sum_{n'=1}^N q(l_{n'} = k) \mathbf{u}_{n'} \right) \left(\mathbf{u}_n - \frac{1}{N_k} \sum_{n'=1}^N q(l_{n'} = k) \mathbf{u}_{n'} \right)^T \quad (\text{A15})$$

$$+ \frac{\lambda_k N_k}{\lambda_k + N_k} \left(\frac{1}{N_k} \sum_{n'=1}^N q(l_{n'} = k) \mathbf{u}_{n'} - \boldsymbol{\mu}_k \right) \left(\frac{1}{N_k} \sum_{n'=1}^N q(l_{n'} = k) \mathbf{u}_{n'} - \boldsymbol{\mu}_k \right)^T$$

$$q(l_n = k) = \frac{\rho_{nk}^*}{\sum_{i=1}^M \rho_{ni}^*} \quad (\text{A16})$$

where ρ_{nk}^* is defined as follows.

$$\rho_{nk}^* = \exp \left\{ \langle \ln \beta_k \rangle + \sum_{i=1}^{k-1} \langle \ln(1 - \beta_i) \rangle + \frac{1}{2} \langle \ln |\mathbf{H}_k| \rangle - \frac{K}{2} \ln 2\pi - \frac{1}{2} \langle (\mathbf{u}_n - \boldsymbol{\eta}_k)^T \mathbf{H}_k (\mathbf{u}_n - \boldsymbol{\eta}_k) \rangle \right\} \quad (\text{A17})$$

where $K = \dim(\mathbf{u})$ is the dimension of uncertainty data.

The expressions involved $\langle \cdot \rangle$ are listed below.

$$\langle \alpha \rangle = \frac{\lambda_1^*}{\lambda_2^*} \quad (\text{A18})$$

$$\langle \ln \beta_k \rangle = \psi(\tau_k) - \psi(\tau_k + \nu_k) \quad (\text{A19})$$

$$\langle \ln(1 - \beta_k) \rangle = \psi(\nu_k) - \psi(\tau_k + \nu_k) \quad (\text{A20})$$

$$\langle \ln |\mathbf{H}_k| \rangle = \sum_{i=1}^K \psi \left(\frac{\omega_k^* + 1 - i}{2} \right) + K \ln 2 - \ln |\Psi_k^*| \quad (\text{A21})$$

$$\langle (\mathbf{u}_n - \boldsymbol{\eta}_k)^T \mathbf{H}_k (\mathbf{u}_n - \boldsymbol{\eta}_k) \rangle = \frac{K}{\lambda_k} + \omega_k (\mathbf{u}_n - \boldsymbol{\mu}_k^*)^T \Psi_k^{\omega_k - 1} (\mathbf{u}_n - \boldsymbol{\mu}_k^*) \quad (\text{A22})$$

where ψ is the digamma function.

The variational inference algorithm is summarized below.

Algorithm. Variational inference algorithm

- 1: Input uncertainty data set $\mathbf{U} = \{\mathbf{u}_n\}_{n=1}^N$;
 - 2: Set ζ_e and $q(\mathbf{l}, \boldsymbol{\beta}, \alpha, \boldsymbol{\eta}, \mathbf{H})$;
 - 3: **while** $\left| \frac{\text{ELBO}_t(q) - \text{ELBO}_{t-1}(q)}{\text{ELBO}_{t-1}(q)} \right| \geq \zeta_e$ **do**
 - 4: Update $q(\alpha)$ by the expression in (A4);
 - 5: **for** $k=1$ to M **do**
 - 6: Update $q(\beta_k)$ by the expression in (A7);
 - 7: Update $q(\boldsymbol{\eta}_k, \mathbf{H}_k)$ by the expression in (A10);
 - 8: **end**
 - 9: **for** $n=1$ to N **do**
 - 10: Update $q(l_n)$ by the expression in (A16);
 - 11: **end**
 - 12: **end**
 - 13: Output $q(\mathbf{l}, \boldsymbol{\beta}, \alpha, \boldsymbol{\eta}, \mathbf{H}) = \prod_{i=1}^N q(l_i) \prod_{k=1}^{M-1} q(\beta_k) q(\alpha) \prod_{k=1}^M q(\boldsymbol{\eta}_k, \mathbf{H}_k)$
-

Figure A1. The variational inference algorithm for the Dirichlet process mixture model.

Appendix B. Supplementary Data for Case Study 1

Table B1. Mass balance relationships for processes in case study 1.

Process	Mass balance relationship
Process 1	0.63 A + 0.58 C → E
Process 2	0.64 A → D
Process 3	1.25 B → 0.9 C + E

Table B2. Fixed investment costs (10^2 \$) for processes in case study 1.

Process	Period 1	Period 2	Period 3	Period 4	Period 5	Period 6	Period 7	Period 8	Period 9	Period 10
Process 1	337.0	260.0	200.0	150.0	120.0	80.0	70.0	90.0	120.0	150.0
Process 2	125.0	120.0	101.0	121.0	121.0	125.0	120.0	101.0	141.0	181.0
Process 3	61.0	61.0	30.0	20.0	15.0	50.0	51.0	40.0	20.0	60.0

Table B3. Variable investment costs (10^2 \$/t) for processes in case study 1.

Process	Period 1	Period 2	Period 3	Period 4	Period 5	Period 6	Period 7	Period 8	Period 9	Period 10
Process 1	3.7	3.6	4.0	2.0	1.0	2.2	2.6	2.5	2.4	3.0
Process 2	2.5	2.4	2.9	5.2	3.0	1.5	2.4	2.9	2.2	4.0
Process 3	3.1	3.0	3.3	2.4	2.0	1.1	3.0	3.3	2.4	2.0

Table B4. Purchase prices (10^2 \$/t) for chemicals in case study 1.

Chemicals	Period 1	Period 2	Period 3	Period 4	Period 5	Period 6	Period 7	Period 8	Period 9	Period 10
A	8.2	9.0	5.5	5.0	5.2	4.2	3.0	4.5	3.0	5.0
B	4.0	3.3	3.2	2.0	2.0	2.0	3.3	2.2	3.0	2.0
C	1.5	1.3	1.2	1.1	1.2	1.5	1.3	1.2	1.1	1.2
D	0.0	0.0	0.0	0.0	0.0	0.0	0.0	0.0	0.0	0.0
E	0.0	0.0	0.0	0.0	0.0	0.0	0.0	0.0	0.0	0.0

Table B5. Sale prices (10^2 \$/t) for chemicals in case study 1.

Chemicals	Period 1	Period 2	Period 3	Period 4	Period 5	Period 6	Period 7	Period 8	Period 9	Period 10
A	0.0	0.0	0.0	0.0	0.0	0.0	0.0	0.0	0.0	0.0
B	0.0	0.0	0.0	0.0	0.0	0.0	0.0	0.0	0.0	0.0
C	0.0	0.0	0.0	0.0	0.0	0.0	0.0	0.0	0.0	0.0
D	15.4	14.0	16.5	17.3	18.5	22.4	32.0	34.5	21.3	22.5
E	12.8	12.0	15.0	18.0	25.0	28.8	23.0	21.0	22.0	22.0

Table B6. Operating costs (10^2 \$/t) for processes in case study 1.

Process	Period 1	Period 2	Period 3	Period 4	Period 5	Period 6	Period 7	Period 8	Period 9	Period 10
Process 1	0.8	0.5	0.4	0.6	0.4	0.3	0.3	0.4	0.3	0.3
Process 2	1.5	1.6	1.5	1.0	1.0	0.8	0.6	0.5	1.0	1.0
Process 3	1.5	1.2	1.0	0.8	0.8	0.9	1.5	1.2	0.8	1.5

Appendix C. Supplementary Data for Case Study 2

Table C1. Mass balance relationships for processes in case study 2.

Process	Mass balance relationship	Process	Mass balance relationship
Process 1	$0.58 A + 0.63 F \rightarrow K$	Process 20	$0.35 D + 0.71 T \rightarrow U$
Process 2	$0.64 F \rightarrow L$	Process 21	$0.32 F + 0.72 T \rightarrow U$
Process 3	$1.25 B \rightarrow 0.055 A + K$	Process 22	$0.88 D \rightarrow E + 0.03 X$
Process 4	$0.4 B + 0.69 C \rightarrow N$	Process 23	$0.56 A + 0.92 E \rightarrow K$
Process 5	$2.3 N \rightarrow M + 1.7 Q$	Process 24	$0.39 D \rightarrow AB$
Process 6	$0.74 B \rightarrow O$	Process 25	$1.97 AB \rightarrow E$
Process 7	$1.1 O \rightarrow M$	Process 26	$0.3 D \rightarrow W$
Process 8	$C \rightarrow P$	Process 27	$0.65 T + 0.46 AB \rightarrow V$
Process 9	$1.26 P \rightarrow Q$	Process 28	$0.56 G + 0.56 J \rightarrow T$
Process 10	$1.57 M \rightarrow AA$	Process 29	$1.2 L \rightarrow V$
Process 11	$1.01 C \rightarrow Q$	Process 30	$1.17 D \rightarrow Y$
Process 12	$0.76 C + 0.28 D \rightarrow H$	Process 31	$0.75 E \rightarrow X$
Process 13	$1.14 H \rightarrow R$	Process 32	$0.53 D \rightarrow X$
Process 14	$0.78 B \rightarrow M$	Process 33	$0.6 L + 0.82 T \rightarrow U$
Process 15	$1.34 S \rightarrow L$	Process 34	$0.42 J \rightarrow Y$
Process 16	$0.6 D \rightarrow S$	Process 35	$0.5 I \rightarrow J$
Process 17	$0.67 D \rightarrow L$	Process 36	$0.53 G + 0.57 Y \rightarrow X$
Process 18	$1.1 L \rightarrow T$	Process 37	$1.44 AB \rightarrow X$
Process 19	$0.98 S \rightarrow T$	Process 38	$3.08 I \rightarrow 0.38 B + 0.22 C + D$

Table C2. Fixed investment costs (10⁵ \$) for processes in case study 2.

Process	Period 1	Period 2	Period 3	Period 4	Period 5	Period 6	Period 7	Period 8	Period 9	Period 10
Process 1	337.1	260.0	200.0	150.0	120.0	50.0	60.0	30.0	150.0	150.0
Process 2	125.0	120.0	101.0	121.0	121.0	125.0	20.0	101.0	41.0	81.0
Process 3	321.0	311.0	300.0	200.0	250.0	121.0	111.0	100.0	100.0	150.0
Process 4	80.8	71.0	66.0	77.0	77.0	80.8	21.0	66.0	77.0	77.0
Process 5	96.6	90.0	85.0	84.0	84.0	96.6	20.0	85.0	84.0	84.0
Process 6	162.0	60.0	55.0	43.0	43.0	162.0	60.0	15.0	43.0	43.0
Process 7	105.0	98.0	67.0	56.0	56.0	105.0	98.0	17.0	56.0	56.0
Process 8	102.0	82.0	73.0	60.0	80.0	102.0	82.0	83.0	110.0	110.0
Process 9	115.0	105.0	145.0	140.0	140.0	15.0	15.0	145.0	140.0	140.0
Process 10	17.5	16.0	23.0	21.0	21.0	17.5	16.0	23.0	21.0	21.0
Process 11	118.0	107.0	118.0	109.0	109.0	18.0	107.0	18.0	19.0	19.0
Process 12	50.0	40.0	50.0	150.0	50.0	50.0	40.0	50.0	150.0	50.0
Process 13	237.0	227.0	238.0	241.0	241.0	137.0	127.0	138.0	141.0	141.0
Process 14	52.9	54.0	40.0	30.0	30.0	52.9	54.0	40.0	30.0	30.0
Process 15	120.0	113.0	114.0	101.0	114.0	120.0	113.0	114.0	101.0	114.0
Process 16	37.0	40.0	51.0	60.0	60.0	37.0	40.0	51.0	60.0	60.0
Process 17	110.0	120.0	101.0	98.0	101.0	110.0	120.0	101.0	98.0	101.0
Process 18	40.0	50.0	48.0	32.0	32.0	40.0	50.0	48.0	32.0	32.0
Process 19	42.0	43.0	40.0	20.0	40.0	42.0	43.0	40.0	20.0	40.0
Process 20	75.0	60.0	54.0	50.0	50.0	75.0	60.0	54.0	50.0	50.0
Process 21	75.0	60.0	50.0	60.0	60.0	75.0	60.0	50.0	60.0	60.0
Process 22	101.0	100.0	92.0	81.0	81.0	101.0	100.0	92.0	81.0	81.0
Process 23	353.0	342.0	350.0	291.0	291.0	353.0	342.0	350.0	291.0	291.0
Process 24	150.0	140.0	120.0	141.0	141.0	150.0	140.0	120.0	141.0	141.0
Process 25	130.0	120.0	143.0	122.0	122.0	130.0	120.0	143.0	122.0	122.0
Process 26	85.0	75.0	68.0	71.0	71.0	85.0	75.0	68.0	71.0	71.0
Process 27	25.0	14.0	21.0	19.0	21.0	25.0	14.0	21.0	19.0	21.0
Process 28	61.0	32.0	34.0	29.0	19.0	11.0	12.0	10.0	9.0	10.0
Process 29	27.0	16.0	16.0	18.0	18.0	27.0	16.0	16.0	18.0	18.0
Process 30	120.0	118.0	116.0	119.0	119.0	120.0	118.0	116.0	119.0	119.0
Process 31	87.0	90.0	81.0	80.0	80.0	87.0	90.0	81.0	80.0	80.0
Process 32	85.0	91.0	89.0	80.0	80.0	85.0	91.0	89.0	80.0	80.0
Process 33	80.0	70.0	61.0	52.0	52.0	80.0	70.0	61.0	52.0	52.0
Process 34	111.0	100.0	80.0	80.0	80.0	111.0	100.0	80.0	80.0	80.0
Process 35	54.0	60.0	45.0	43.0	43.0	54.0	60.0	45.0	43.0	43.0
Process 36	89.0	91.0	90.0	100.0	100.0	89.0	91.0	90.0	100.0	40.0
Process 37	131.0	120.0	100.0	151.0	100.0	31.0	20.0	100.0	51.0	40.0
Process 38	12.8	9.0	8.0	4.0	9.0	12.8	9.0	8.0	4.0	9.0

Table C3. Variable investment costs (10^2 \$/t) for processes in case study 2.

Process	Period 1	Period 2	Period 3	Period 4	Period 5	Period 6	Period 7	Period 8	Period 9	Period 10
Process 1	3.7	3.6	4.0	2.0	1.0	0.2	0.6	0.5	0.4	3.0
Process 2	2.5	2.4	2.9	5.2	3.0	1.5	0.4	2.9	0.2	4.0
Process 3	3.1	3.0	3.3	0.4	2.0	0.1	3.0	3.3	4.4	2.0
Process 4	1.0	0.5	0.5	0.6	0.5	0.2	0.5	0.1	0.1	0.1
Process 5	2.1	2.0	2.0	0.1	1.0	1.1	2.0	1.0	2.1	1.0
Process 6	3.8	0.6	0.4	0.6	1.0	1.8	0.6	0.2	0.6	1.0
Process 7	1.3	1.0	0.5	0.5	1.0	0.3	1.0	0.2	0.5	1.0
Process 8	0.5	0.5	0.6	0.2	0.2	0.2	0.2	0.1	0.9	1.0
Process 9	1.5	1.2	0.8	1.0	1.0	1.5	0.2	0.2	1.0	0.9
Process 10	0.9	0.5	0.4	1.2	1.0	0.9	0.5	0.1	1.2	0.8
Process 11	1.7	1.6	1.5	1.8	1.0	1.1	0.6	0.1	1.8	1.0
Process 12	0.6	0.4	0.2	0.4	0.3	0.1	0.4	0.2	0.4	0.6
Process 13	3.0	1.5	1.5	1.6	1.2	0.1	0.5	1.5	1.6	0.4
Process 14	0.5	1.0	0.5	0.2	0.3	0.1	1.0	0.3	0.2	0.2
Process 15	2.0	1.0	1.1	0.4	0.8	1.0	1.0	0.1	0.1	1.0
Process 16	0.8	0.4	0.6	0.7	0.5	0.8	0.4	0.3	0.7	0.5
Process 17	0.8	1.4	1.9	0.8	0.5	0.8	0.4	0.9	0.8	0.2
Process 18	1.9	1.5	2.0	2.0	1.0	0.9	0.5	1.0	1.0	1.0
Process 19	2.5	2.0	2.4	2.2	2.0	2.5	2.0	0.4	2.2	1.0
Process 20	2.4	2.5	2.0	0.8	2.0	0.4	0.5	1.0	0.8	1.0
Process 21	2.4	2.5	1.8	0.9	1.0	0.4	0.5	0.8	0.9	0.4
Process 22	5.8	6.0	5.5	6.0	3.0	0.8	6.0	0.5	2.0	3.0
Process 23	4.0	2.5	2.0	2.0	3.0	2.0	0.5	1.0	1.0	1.0
Process 24	3.0	3.2	3.1	3.1	2.0	2.0	2.2	0.1	1.1	2.0
Process 25	2.5	2.0	1.8	1.8	2.0	1.5	2.0	0.2	1.8	1.0
Process 26	1.5	1.0	0.5	0.5	1.0	0.5	1.0	0.5	0.5	1.0
Process 27	0.8	0.4	0.2	0.4	0.2	0.8	0.4	0.1	0.4	0.5
Process 28	2.0	0.7	0.9	0.8	1.0	0.2	0.1	0.1	0.1	0.1
Process 29	0.9	1.9	1.8	0.9	1.0	0.9	0.9	0.8	0.9	1.0
Process 30	3.0	3.0	2.5	2.2	1.0	1.0	1.0	0.5	0.2	1.0
Process 31	3.9	3.0	2.0	2.1	1.0	0.9	1.0	1.0	1.1	1.0
Process 32	1.5	3.0	2.4	1.0	1.0	0.2	0.3	0.4	2.0	1.0
Process 33	0.9	1.0	5.0	2.5	1.0	0.1	1.0	1.0	2.5	1.0
Process 34	1.6	1.5	0.9	0.9	1.0	0.1	0.1	0.1	0.1	1.0
Process 35	1.7	2.0	1.0	1.0	2.0	0.2	0.1	0.1	1.0	1.0
Process 36	4.3	3.0	1.0	1.1	2.0	0.1	0.2	1.0	1.1	1.0
Process 37	6.8	6.5	6.0	6.2	5.0	0.8	0.5	2.0	0.2	1.0
Process 38	0.9	0.5	0.3	0.4	0.8	0.1	0.5	0.3	0.4	1.0

Table C4. Purchase prices (10^2 \$/t) for chemicals in case study 2.

Chemicals	Period 1	Period 2	Period 3	Period 4	Period 5	Period 6	Period 7	Period 8	Period 9	Period 10
A	8.2	9.0	5.5	8.0	8.0	8.2	9.0	5.5	8.0	8.0
B	4.0	3.3	4.2	4.0	4.0	4.0	3.3	4.2	4.0	4.0
C	4.4	5.5	3.0	2.0	3.0	4.4	5.5	3.0	2.0	3.0
D	3.5	3.3	3.2	3.1	3.2	3.5	3.3	3.2	3.1	3.2
E	8.6	8.8	8.0	7.5	8.0	8.6	8.8	8.0	7.5	8.0
F	5.5	6.0	6.2	5.0	6.2	5.5	6.0	6.2	5.0	6.2
G	0.4	0.3	1.0	1.1	0.8	0.4	0.3	1.0	1.1	0.8
H	6.6	6.1	7.0	5.0	6.0	6.6	6.1	7.0	5.0	6.0
I	4.1	5.2	5.8	4.0	5.0	4.1	5.2	5.8	4.0	5.0
J	2.6	2.5	3.0	2.2	2.5	2.6	2.5	3.0	2.2	2.5
K	0.0	0.0	0.0	0.0	0.0	0.0	0.0	0.0	0.0	0.0
L	0.0	0.0	0.0	0.0	0.0	0.0	0.0	0.0	0.0	0.0
M	0.0	0.0	0.0	0.0	0.0	0.0	0.0	0.0	0.0	0.0
N	0.0	0.0	0.0	0.0	0.0	0.0	0.0	0.0	0.0	0.0
O	0.0	0.0	0.0	0.0	0.0	0.0	0.0	0.0	0.0	0.0
P	0.0	0.0	0.0	0.0	0.0	0.0	0.0	0.0	0.0	0.0
Q	0.0	0.0	0.0	0.0	0.0	0.0	0.0	0.0	0.0	0.0
R	0.0	0.0	0.0	0.0	0.0	0.0	0.0	0.0	0.0	0.0
S	0.0	0.0	0.0	0.0	0.0	0.0	0.0	0.0	0.0	0.0
T	0.0	0.0	0.0	0.0	0.0	0.0	0.0	0.0	0.0	0.0
U	0.0	0.0	0.0	0.0	0.0	0.0	0.0	0.0	0.0	0.0
V	0.0	0.0	0.0	0.0	0.0	0.0	0.0	0.0	0.0	0.0
W	0.0	0.0	0.0	0.0	0.0	0.0	0.0	0.0	0.0	0.0
X	0.0	0.0	0.0	0.0	0.0	0.0	0.0	0.0	0.0	0.0
Y	0.0	0.0	0.0	0.0	0.0	0.0	0.0	0.0	0.0	0.0
Z	0.0	0.0	0.0	0.0	0.0	0.0	0.0	0.0	0.0	0.0
AA	0.0	0.0	0.0	0.0	0.0	0.0	0.0	0.0	0.0	0.0
AB	0.0	0.0	0.0	0.0	0.0	0.0	0.0	0.0	0.0	0.0

Table C5. Sale prices (10^2 \$/t) for chemicals in case study 2.

Chemicals	Period 1	Period 2	Period 3	Period 4	Period 5	Period 6	Period 7	Period 8	Period 9	Period 10
A	0.0	0.0	0.0	0.0	0.0	0.0	0.0	0.0	0.0	0.0
B	0.0	0.0	0.0	0.0	0.0	0.0	0.0	0.0	0.0	0.0
C	0.0	0.0	0.0	0.0	0.0	0.0	0.0	0.0	0.0	0.0
D	0.0	0.0	0.0	0.0	0.0	0.0	0.0	0.0	0.0	0.0
E	0.0	0.0	0.0	0.0	0.0	0.0	0.0	0.0	0.0	0.0
F	0.0	0.0	0.0	0.0	0.0	0.0	0.0	0.0	0.0	0.0
G	0.0	0.0	0.0	0.0	0.0	0.0	0.0	0.0	0.0	0.0
H	0.0	0.0	0.0	0.0	0.0	0.0	0.0	0.0	0.0	0.0
I	0.0	0.0	0.0	0.0	0.0	0.0	0.0	0.0	0.0	0.0
J	0.0	0.0	0.0	0.0	0.0	0.0	0.0	0.0	0.0	0.0
K	8.4	9.9	8.0	7.5	7.5	8.4	9.9	8.0	7.5	7.5
L	6.3	7.0	6.5	6.4	6.4	6.3	7.0	6.5	6.4	6.4
M	6.4	7.2	7.0	8.6	7.0	6.4	7.2	7.0	8.6	7.0
N	5.5	5.4	3.0	2.5	4.5	5.5	5.4	3.0	2.5	4.5
O	5.4	4.0	3.5	3.3	4.5	5.4	4.0	3.5	3.3	4.5
P	12.8	12.0	11.0	10.0	10.0	12.8	12.0	11.0	10.0	10.0
Q	7.3	5.0	4.0	3.3	4.0	7.3	5.0	4.0	3.3	4.0
R	7.5	6.0	5.0	4.5	4.5	7.5	6.0	5.0	4.5	4.5
S	6.1	7.5	7.0	6.2	7.2	6.1	7.5	7.0	6.2	7.2
T	5.4	5.0	8.0	8.2	6.4	5.4	5.0	8.0	8.2	6.4
U	7.4	7.0	4.0	4.1	5.6	7.4	7.0	4.0	4.1	5.6
V	7.9	3.0	3.2	3.1	4.5	7.9	3.0	3.2	3.1	4.5
W	3.1	2.0	1.8	1.0	1.2	3.1	2.0	1.8	1.0	1.2
X	7.5	8.0	7.5	9.0	7.8	7.5	8.0	7.5	9.0	7.8
Y	1.6	1.4	1.3	1.3	1.5	1.6	1.4	1.3	1.3	1.5
Z	3.3	4.0	4.1	1.5	3.8	3.3	4.0	4.1	1.5	3.8
AA	0.0	0.0	0.0	0.0	0.0	0.0	0.0	0.0	0.0	0.0
AB	0.0	0.0	0.0	0.0	0.0	0.0	0.0	0.0	0.0	0.0

Table C6. Operating costs (10^2 \$/t) for processes in case study 2.

Process	Period 1	Period 2	Period 3	Period 4	Period 5	Period 6	Period 7	Period 8	Period 9	Period 10
Process 1	0.8	0.5	0.4	0.6	0.6	0.8	0.5	0.4	0.6	0.6
Process 2	1.5	1.6	1.5	2.0	2.0	1.5	1.6	1.5	2.0	2.0
Process 3	1.0	1.2	1.0	1.8	1.8	1.0	1.2	1.0	1.8	1.8
Process 4	1.1	1.0	0.8	1.8	1.8	1.1	1.0	0.8	1.8	1.8
Process 5	1.1	0.8	0.6	0.5	0.5	1.1	0.8	0.6	0.5	0.5
Process 6	0.7	0.5	0.6	0.9	0.9	0.7	0.5	0.6	0.9	0.9
Process 7	1.0	0.7	0.5	0.9	0.9	1.0	0.7	0.5	0.9	0.9
Process 8	2.5	2.0	1.8	2.0	2.0	2.5	2.0	1.8	2.0	2.0
Process 9	1.5	1.5	1.4	1.0	1.0	1.5	1.5	1.4	1.0	1.0
Process 10	2.0	1.8	1.6	0.5	1.6	2.0	1.8	1.6	0.5	1.6
Process 11	2.0	1.8	1.8	0.9	1.8	2.0	1.8	1.8	0.9	1.8
Process 12	0.7	0.5	0.4	0.4	0.5	0.7	0.5	0.4	0.4	0.5
Process 13	0.7	0.6	0.6	0.6	0.6	0.7	0.6	0.6	0.6	0.6
Process 14	2.0	2.0	1.8	0.9	1.8	0.01	0.01	1.8	0.9	1.8
Process 15	1.6	1.5	1.4	1.5	1.5	0.6	1.5	1.4	1.5	1.5
Process 16	1.0	1.2	1.0	1.2	1.2	1.0	1.2	1.0	1.2	1.2
Process 17	1.3	1.0	0.9	0.1	1.0	1.3	1.0	0.9	0.1	1.0
Process 18	0.8	0.4	0.2	0.2	0.4	0.8	0.4	0.2	0.2	0.4
Process 19	1.5	1.0	1.1	1.0	1.0	1.5	1.0	1.1	1.0	1.0
Process 20	2.5	2.0	2.1	2.2	2.1	2.5	2.0	2.1	2.2	2.1
Process 21	3.0	3.0	2.7	2.8	2.8	3.0	3.0	2.7	2.8	2.8
Process 22	1.5	1.2	1.0	0.9	0.9	1.5	1.2	1.0	0.9	0.9
Process 23	1.3	1.0	0.8	0.1	0.8	1.3	1.0	0.8	0.1	0.8
Process 24	2.0	1.5	1.4	1.0	1.0	2.0	1.5	1.4	1.0	1.0
Process 25	2.3	2.0	1.8	1.9	1.8	2.3	2.0	1.8	1.9	1.8
Process 26	1.0	1.1	1.0	0.9	1.0	1.0	1.1	1.0	0.9	1.0
Process 27	1.5	1.0	0.8	0.6	0.8	1.5	1.0	0.8	0.6	0.8
Process 28	1.0	0.8	0.7	0.7	0.7	1.0	0.8	0.7	0.7	0.7
Process 29	2.0	1.8	1.9	1.9	1.6	2.0	1.8	1.9	1.9	1.6
Process 30	2.0	1.9	1.7	1.6	1.6	2.0	1.9	1.7	1.6	1.6
Process 31	3.0	2.5	2.0	1.6	1.0	3.0	2.5	2.0	1.6	1.0
Process 32	2.0	1.9	2.0	1.0	1.0	2.0	1.9	2.0	1.0	1.0
Process 33	3.0	3.1	3.2	3.1	3.1	3.0	3.1	3.2	3.1	3.1
Process 34	0.4	0.3	0.2	0.4	0.4	0.4	0.3	0.2	0.4	0.4
Process 35	1.3	1.2	1.1	0.1	1.1	1.3	1.2	1.1	0.1	1.1
Process 36	3.0	2.8	2.4	2.2	2.2	3.0	2.8	2.4	2.2	2.2
Process 37	3.5	3.0	2.5	3.0	3.0	3.5	3.0	2.5	3.0	3.0
Process 38	1.0	1.2	1.0	1.1	1.1	1.0	1.2	1.0	1.1	1.1

Notation

DDNSRO Framework

The main notations used in the DDNSRO modeling framework are listed below.

b	vector of objective coefficients corresponding to second-stage decisions
c	vector of objective coefficients corresponding to first-stage decisions
u	vector of uncertainties
x	vector of first-stage decisions
y_s	vector of second-stage decisions for data class <i>s</i>
μ_k	vector of parameters in normal Wishart distribution
η_k	mean vector in the Dirichlet process mixture model of Gaussian distributions
C	total number of data classes in uncertainty data
l_i	index of mixture components assigned to the observation <i>o_i</i>
m(<i>s</i>)	total number of basic uncertainty sets for data class <i>s</i>
M	truncation level in the Variational inference
M₀	constant with a very large value
U_s	uncertainty set for data class <i>s</i>
o_i	the observation generated from the Dirichlet process mixture model
s	index of data class
α	concentration parameter in the Dirichlet process
λ_k	parameter in normal Wishart distribution
θ_k	random variable drawn from the base distribution
π_k	parameter of weight in the Dirichlet process
ω_i	parameter in normal Wishart distribution
β_k	proportion of stick being broken from the remaining stick
Λ_i	scaling factor in the data-driven uncertainty set
τ_i	a hyper-parameter for Beta distribution in the Variational inference
v_i	a hyper-parameter for Beta distribution in the Variational inference

γ_i	weight of mixture component
γ^*	threshold value for the weight of mixture component
Θ	support of the base distribution
F_0	base distribution in the Dirichlet process
$\Phi_{s,i}$	uncertainty budget in data-driven uncertainty set
\mathbf{A}	coefficient matrix corresponding to the first-stage decisions
\mathbf{H}_k	precision matrix in the Dirichlet process mixture model of Gaussian distributions
\mathbf{M}	coefficient matrix corresponding to the uncertainties
\mathbf{T}	technology matrix in the DDNSRO framework
\mathbf{W}	recourse matrix in the DDNSRO framework
Ψ_k	parameter in the normal Wishart distribution

Application to planning of process networks

The sets, parameters, and variables used in the application part are summarized below. Note that all parameters are denoted in lower-case symbols, and all variables are denoted in upper-case symbols.

Sets/indices

I	set of processes indexed by i
J	set of chemicals indexed by j
T	set of time periods indexed by t
Ξ	set of data classes indexed by s

Parameters

ce_i	maximum number of expansions for process i over the planning horizon
du_{jt}	demand of chemical j in time period t
su_{jt}	supply of chemical j in time period t
$c1_{it}$	variable investment cost for process i in time period t
$c2_{it}$	fixed investment cost for process i in time period t
$c3_{it}$	unit operating cost for process i in time period t
$c4_{it}$	purchase price of chemical j in time period t

cb_t	maximum allowable investment in time period t
qe_{it}^L	lower bound for capacity expansion of process i in time period t
qe_{it}^U	upper bound for capacity expansion of process i in time period t
v_{jt}	sale price of chemical j in time period t
κ_{ij}	mass balance coefficient for chemical j in process i

Binary variables

Y_{it}	binary variable that indicates whether process i is chosen for expansion in time period t
----------	---

Continuous variables

P_{sjt}	purchase amount of chemical j in time period t for data class s
Q_{it}	total capacity of process i in time period t
QE_{it}	capacity expansion of process i in time period t
SA_{sjt}	sale amount of chemical j in time period t for data class s
W_{sit}	operation level of process i in time period t for data class s

Literature Cited

1. Sahinidis NV. Optimization under uncertainty: State-of-the-art and opportunities. *Comput. Chem. Eng.* 2004;28(6–7):971-983.
2. Grossmann IE, Apap RM, Calfa BA, García-Herreros P, Zhang Q. Recent advances in mathematical programming techniques for the optimization of process systems under uncertainty. *Comput. Chem. Eng.* 2016;91:3-14.
3. Pistikopoulos EN. Uncertainty in process design and operations. *Comput. Chem. Eng.* 1995;19:553-563.
4. Mulvey JM, Vanderbei RJ, Zenios SA. Robust Optimization of Large-Scale Systems. *Oper. Res.* 1995;43(2):264-281.
5. Ben-Tal A, Nemirovski A. Robust optimization – methodology and applications. *Math. Program.* 2002;92(3):453-480.
6. Birge JR, Louveaux F. *Introduction to stochastic programming*: Springer Science & Business Media; 2011.
7. Gabrel V, Murat C, Thiele A. Recent advances in robust optimization: An overview. *Eur. J. Oper. Res.* 2014;235(3):471-483.
8. Bertsimas D, Brown DB, Caramanis C. Theory and applications of robust optimization. *SIAM Rev.* 2011;53(3):464-501.
9. Gong J, Garcia DJ, You F. Unraveling Optimal Biomass Processing Routes from Bioconversion Product and Process Networks under Uncertainty: An Adaptive Robust Optimization Approach. *ACS Sustain. Chem. Eng.* 2016;4(6):3160-3173.

10. Gong J, You F. Optimal processing network design under uncertainty for producing fuels and value-added bioproducts from microalgae: Two-stage adaptive robust mixed integer fractional programming model and computationally efficient solution algorithm. *AIChE J.* 2017;63(2):582-600.
11. Shi H, You F. A computational framework and solution algorithms for two-stage adaptive robust scheduling of batch manufacturing processes under uncertainty. *AIChE J.* 2016;62(3):687-703.
12. Gao J, You F. Deciphering and handling uncertainty in shale gas supply chain design and optimization: Novel modeling framework and computationally efficient solution algorithm. *AIChE J.* 2015;61(11):3739-3755.
13. Chu Y, You F. Integration of Scheduling and Dynamic Optimization of Batch Processes under Uncertainty: Two-Stage Stochastic Programming Approach and Enhanced Generalized Benders Decomposition Algorithm. *Ind. Eng. Chem. Res.* 2013;52(47):16851-16869.
14. Kasivisvanathan H, Ubando AT, Ng DKS, Tan RR. Robust optimization for process synthesis and design of multifunctional energy systems with uncertainties. *Ind. Eng. Chem. Res.* 2014;53(8):3196-3209.
15. Cardoso SR, Barbosa-Póvoa APFD, Relvas S. Design and planning of supply chains with integration of reverse logistics activities under demand uncertainty. *Eur. J. Oper. Res.* 2013;226(3):436-451.
16. Liu S, Farid SS, Papageorgiou LG. Integrated Optimization of Upstream and Downstream Processing in Biopharmaceutical Manufacturing under Uncertainty: A Chance Constrained Programming Approach. *Ind. Eng. Chem. Res.* 2016;55(16):4599-4612.
17. Birge JR. State-of-the-Art-Survey—Stochastic Programming: Computation and Applications. *INFORMS J. Comput.* 1997;9(2):111-133.
18. Bonfill A, Espuña A, Puigjaner L. Addressing Robustness in Scheduling Batch Processes with Uncertain Operation Times. *Ind. Eng. Chem. Res.* 2005;44(5):1524-1534.
19. Bonfill A, Bagajewicz M, Espuña A, Puigjaner L. Risk Management in the Scheduling of Batch Plants under Uncertain Market Demand. *Ind. Eng. Chem. Res.* 2004;43(3):741-750.
20. Liu P, Pistikopoulos EN, Li Z. Decomposition Based Stochastic Programming Approach for Polygeneration Energy Systems Design under Uncertainty. *Ind. Eng. Chem. Res.* 2010;49(7):3295-3305.
21. Gebreslassie BH, Yao Y, You F. Design under uncertainty of hydrocarbon biorefinery supply chains: Multiobjective stochastic programming models, decomposition algorithm, and a Comparison between CVaR and downside risk. *AIChE J.* 2012;58(7):2155-2179.
22. Zeballos LJ, Méndez CA, Barbosa-Povoa AP. Design and Planning of Closed-Loop Supply Chains: A Risk-Averse Multistage Stochastic Approach. *Ind. Eng. Chem. Res.* 2016;55(21):6236-6249.
23. Yuan Y, Li Z, Huang B. Robust optimization under correlated uncertainty: Formulations and computational study. *Comput. Chem. Eng.* 2016;85:58-71.
24. Ben-Tal A, Nemirovski A. Robust solutions of Linear Programming problems contaminated with uncertain data. *Math. Programming.* 2000;88:411.
25. Bertsimas D, Sim M. The price of robustness. *Oper. Res.* 2004;52(1):35.
26. Ben-Tal A, Ghaoui LE, Nemirovski A. *Robust Optimization*: Princeton University Press; 2009.

27. Li Z, Ding R, Floudas CA. A Comparative Theoretical and Computational Study on Robust Counterpart Optimization: I. Robust Linear Optimization and Robust Mixed Integer Linear Optimization. *Ind. Eng. Chem. Res.* 2011;50(18):10567-10603.
28. McLean K, Li X. Robust Scenario Formulations for Strategic Supply Chain Optimization under Uncertainty. *Ind. Eng. Chem. Res.* 2013;52(16):5721-5734.
29. Yue D, You F. Optimal supply chain design and operations under multi-scale uncertainties: Nested stochastic robust optimization modeling framework and solution algorithm. *AIChE J.* 2016;62(9):3041-3055.
30. Liu C, Lee C, Chen H, Mehrotra S. Stochastic Robust Mathematical Programming Model for Power System Optimization. *IEEE Trans. Power Syst.* 2016;31(1):821-822.
31. Jordan MI, Mitchell TM. Machine learning: Trends, perspectives, and prospects. *Science.* 2015;349(6245):255-260.
32. Bertsimas D, Gupta V, Kallus N. Data-driven robust optimization. *Math. Program.* 2017. DOI:10.1007/s10107-017-1125-8
33. Calfa BA, Grossmann IE, Agarwal A, Bury SJ, Wassick JM. Data-driven individual and joint chance-constrained optimization via kernel smoothing. *Comput. Chem. Eng.* 2015;78:51-69.
34. Ning C, You F. Data-driven adaptive nested robust optimization: General modeling framework and efficient computational algorithm for decision making under uncertainty. *AIChE J.* 2017. DOI: 10.1002/aic.15717
35. Jiang R, Guan Y. Data-driven chance constrained stochastic program. *Math. Program.* 2016;158(1):291-327.
36. Shi J, Lee WJ, Liu Y, Yang Y, Wang P. Forecasting Power Output of Photovoltaic Systems Based on Weather Classification and Support Vector Machines. *IEEE Trans. Ind. Appl.* 2012;48(3):1064-1069.
37. Wasserman L. *All of statistics: a concise course in statistical inference*: Springer Science & Business Media; 2013.
38. Murphy KP. *Machine learning: a probabilistic perspective*: MIT press; 2012.
39. Campbell T, How JP. Bayesian nonparametric set construction for robust optimization. Paper presented at: 2015 American Control Conference (ACC); 1-3 July 2015, 2015.
40. Blei DM, Jordan MI. Variational inference for Dirichlet process mixtures. *Bayesian Anal.* 2006;1(1):121-143.
41. Billionnet A, Costa M-C, Poirion P-L. 2-stage robust MILP with continuous recourse variables. *Discrete Appl. Math.* 2014;170:21-32.
42. Zeng B, Zhao L. Solving two-stage robust optimization problems using a column-and-constraint generation method. *Oper. Res. Lett.* 2013;41(5):457-461.
43. Teh WY. Dirichlet Process. In: Sammut C, Webb GI, eds. *Encyclopedia of Machine Learning*. Boston, MA: Springer US; 2010:280-287.
44. Sethuraman J. A constructive definition of Dirichlet priors. *Statistica Sinica.* 1994;4(2):639-650.
45. Blei DM, Jordan MI. Variational inference for Dirichlet process mixtures. 2006:121-143.
46. Kurihara K, Welling M, Vlassis NA. Accelerated variational Dirichlet process mixtures. Paper presented at: Advances in neural information processing systems2006.
47. Takeda A, Taguchi S, Tütüncü RH. Adjustable Robust Optimization Models for a Nonlinear Two-Period System. *Journal of Optimization Theory and Applications.* 2008;136(2):275-295.

48. Bertsimas D, Litvinov E, Sun XA, Zhao J, Zheng T. Adaptive Robust Optimization for the Security Constrained Unit Commitment Problem. *IEEE Trans. Power Syst.* 2013;28(1):52-63.
49. Thiele A, Terry T, Epelman M. Robust linear optimization with recourse. *Tech. Rep.* 2009:4-37.
50. Glover F. Improved linear integer programming formulations of nonlinear integer problems. *Manage. Sci.* 1975;22(4):455-460.
51. You F, Grossmann IE. Multicut Benders decomposition algorithm for process supply chain planning under uncertainty. *Ann. Oper. Res.* 2013;210(1):191-211.
52. Sahinidis NV, Grossmann IE, Fornari RE, Chathrathi M. Optimization model for long range planning in the chemical industry. *Comput. Chem. Eng.* 1989;13(9):1049-1063.
53. You F, Grossmann IE. Stochastic inventory management for tactical process planning under uncertainties: MINLP models and algorithms. *AIChE J.* 2011;57(5):1250-1277.
54. Yue D, You F. Planning and scheduling of flexible process networks under uncertainty with stochastic inventory: MINLP models and algorithm. *AIChE J.* 2013;59(5):1511-1532.
55. Liu ML, Sahinidis NV. Optimization in Process Planning under Uncertainty. *Ind. Eng. Chem. Res.* 1996;35(11):4154-4165.
56. Ahmed S, Sahinidis NV. Robust process planning under uncertainty. *Ind. Eng. Chem. Res.* 1998;37(5):1883-1892.
57. Rosenthal E. *GAMS-A user's guide*. Washington, DC: GAMS Development Corporation; 2008.
58. Wei X, Li C. The infinite Student's t-mixture for robust modeling. *Signal Process.* 2012;92(1):224-234.